SSC JET SPECTROMETER :

A MULTIPURPOSE DETECTOR SCHEME FOR THE CENTRAL REGION*

George E. Theodosiou

Department of Physics
University of Pennsylvania
Philadelphia, Pa. 19104

February 1986

(*) Contribution to the Proceedings of the Workshop on Triggering, Data Acquisition and Computing for High Energy/High Luminosity Hadron -Hadron Colliders, Fermilab, November 11-14 1985.

I. SUMMARY

A large acceptance specialized detector scheme is considered here, which could perform a series of measurements in the central (y=0) region. Its physics goals include the systematic study of jets, bottom-quark and τ-lepton physics and search/study of quark-gluon plasma (QGP) and quark compositeness.

The physics requirements for measurements are defined and various experimental techniques are analyzed with some emphasis on triggering requirements. On this basis a detector scheme is synthesized and various types of triggers are considered. Finally, possible measurements at a higher luminosity (L=10**34/cm**2/sec) are briefly discussed as well as R&D effort needed.

II. MOTIVATION

Our prime motivation for designing this detector is the existence of many physics problems at SSC, which are inaccessible or marginally possible to study with a 4π facility. They could be classified in the following categories:
a) Inaccessible with "conventional" 4π detectors, independent of luminosity: high-Pt direct photons, jet flavor and cascade identification at high Pt, diffractive production etc.
b) Requiring high luminosities, above 10**32/cm**2/sec, but for which measurements are extremely difficult due to high occupancy/cell levels, backgrounds, radiation damage etc, e.g. detailed jet studies above 3-4 TeV, Bottom physics (CP-Violation, Rare decays), etc.
c) Only marginally possible with 4π detectors due to high event complexity and or small cross sections compared to those of background processes, e.g. quark gluon plasma (QGP), Higgs, etc.

Consequently, we have based this study on 2 guiding principles:
a) Focus on the most important physics, which is clearly inaccessible to 4π detectors (otherwise why built it at all).
b) Aim at a self consistent and coherent system structure, whereby the various detector elements and techniques coexist in a logical and cooperative rather than disruptive manner. Examples include the use of calorimeters for precise time as well as energy measurements and a balanced calorimeter design with all its parts subjected to similar signal-to-background ratios.

Several rather simple, very specialized designs already exist. But each one attempts to study just one physics topic such as quark gluon plasma (QGP) or high-Pt hadron production or CP violation or search for heavy particles etc. (Ref.1 to 7). Hence, general reaction has been skeptical (Ref.8):
-Can detector, designed as realistically as possible, perform well enough to do the physics? or
-Cost/Physics output seems too high compared to a general 4π detector or
-How much better can they do it compared to a 4π detector?

It seems no one so far has attempted to come up with a specialized detector scheme for a systematic study of a large fraction of these physics, even though many share some common requirements and therefore one could take advantage of this in detector design to increase physics/cost; e.g. high-Pt direct photons and electrons near jet cores require the best 3-dim calorimeter granularity possible and low tower occupancy levels; the QGP and Bottom physics require high sensitivity to low energy depositions etc.

Here, we propose a drastically different approach:
Design the best possible detector money can buy, optimized for the most demanding measurements: the systematic and detailed study of jets, over the largest possible Pt range and up to the highest possible luminosities. Then a whole range of important physics topics comes automatically within the reach of the detector's capabilities with few improvements or additions.

III. PHYSICS

We concentrate on physics topics that fall almost exclusively in the domain of specialized detectors and most of them have been examined in the past, in different detector schemes. But first we discuss backgrounds:

1. MULTIPLE INTERACTIONS BACKGROUNDS

We attempt crude background estimates from additional interactions occuring within the event time gate for minimum bias and low to medium-Pt constituent scattering. In Appendix 1 we review existing data and extrapolate them to SSC energies and luminosities.

There has been some debate as to the physics behind the increase of $\langle Pt \rangle$ and dN/dy vs. $\sqrt{s}$. UA1 has been able to explain this totally with a relative increase in the fraction of "minijet" events with Et between 5 and 10 GeV, mainly from gg scattering, which at $\sqrt{s}$= 540 GeV are estimated to represent about 12% of the total no. of min.bias events (Ref.55). One could also argue from a naive parton model point of view that this is consistent with the relative increase in the strange particle production, etc. There are others, however, who claim that this may be due to the onset of QGP discussed later.

Trivial background or interesting physics, whatever the explanation might be, the fact remains that increasing transverse energy flux vs $\sqrt{s}$ is present and a detector must be able to deal with it. On the basis of our extrapolations we can estimate background contributions for various trigger gates (Table I):

a) A 10 nsec gate would apply, for example, to a BaF2 calorimeter and affects the electromagnetic triggers. These are possible, down to very low Pt since EM towers are much smaller than 1 str.

b) The 100 nsec gate would apply to scintillating glass (Ref.14) and Pb+gas calorimeters and affects the jet triggers of $D\phi * Dy = 1\text{-}3$ str. Since only about 20-30% of the jet Pt is collected with these calorimeters, we conclude that broad jet triggers are possible above 15 GeV/c but not reliable, until above 30 GeV/c. Here, additional calorimetric timing information might allow reliable jet triggers as low as 10 GeV/c.

c) A 1 μsec gate corresponds to a typical LAr calorimeter. There, isolated electron triggers of relatively low Pt, say above 10-15 GeV/c, would be possible. However we don't see how one can use simple large acceptance triggers for jets reliably with Pt less than 1 TeV/c. With such a slow device, additional triggering requirements for jet triggers would have to be invoked. The low-Pt jet background contribution alone, of Pt= 30 GeV/c, would not be much for a 1 μsec gate, but these are real jets which, if mixed up with an event of interest, can cause trouble both to leptons (μ, electron) and jets of that event of comparable Pt.

2. JET STUDIES: QUARK COMPOSITENESS AND FLAVORS

Here we don't simply mean to measure jet cross section vs Pt, which can be done quite well by a 4π detector anyway. We aim at a series of detailed jet studies for various parton types (gluons, quarks), quark flavors (u,d,s,c,b etc.) vs. parton and jet masses, polarization and other parton parameters as well as initial and final state parton interactions, like gluon or photon bremmstrahlung and weak flavor cascades.

Furthermore, the SSC energy will be at least twenty times higher than any of its predecessors. This will allow us to look at shorter distances and therefore to search for new phenomena. By studying high Pt jet production around 90°, one can test the validity of QCD at the new energy scale, search for quark compositeness, free quarks etc.

Actually these topics have been investigated quite extensively in the last two Workshops at Snowmass (1982, 1984) and elsewhere. In this report we decide to pay more attention to other topics that have not attracted enough attention, in our opinion, so far.

For jet studies we simply mention that the measurements required are: hadron flavor (π /K/p), electron and μ identification from 1 GeV to higher than 1TeV, good EM and hadron calorimetry for electrons/photons/jets from 1 GeV to $\sim$10 TeV.

The triggers required are: dE/dx-Charge (1st Level), Calorimetric EM and Jet (1st-2nd Level), Electron and μ (2nd-3rd Level).

3. DIRECT PHOTON PHYSICS AT HIGH Pt:

a) Probe predictions of conventional QCD and examine compositeness of quarks. Testable scale increasing with luminosity could be as high as 4-5

TeV for L=10**33 to 10**34. A sizeable rate of direct photons of Pt $\sim$ 2TeV for L(tot)= 10**40/cm**2 could be a signature for quark compositeness, as shown in Fig.5b (Ref.33). In QCD, single photons are centrally produced primarily in

$\bar{q}$ q --> g + photon (annihilation) and q g --> q + photon (Compton)

with a flat distribution around y=0 (Ref.32 & 33). Main backgrounds come from Bremmstrahlung of outgoing partons and from leading π^o's in jets (x10**3 for Pt> 1TeV). This would require photon/π^o separations up to energies of several TeV.

We contemplate the need for two spectrometer arms, located around y=0 and back to back in ϕ . The calorimeter in the first arm, pushed back at 7m and of limited acceptance (~3std), emphasizes the high Pt photon detection. The calorimeter in the second arm could be much smaller (cost a small fraction of the main one): if it starts sooner (1.5-2.0m), it could accept the opposite side jet more efficiently (~6std).

b) Photon production in $\bar{q}q'$->W+photon. Measures the trilinear coupling WWγ and hence it may become a sensitive test of deviations from the Standard Model. At SSC its rate drops by x200 by increasing Ptmin(photon) from 20 to 100 GeV/c at y=0. Its θ -angle distribution, with a characteristic dip and symmetry around y=0, is very sensitive to the value of the W magnetic moment, illustrated in Fig.6 (Ref.34),

$$\mu(W) = (1+K) * e / 2 * m(W)$$

Rate(K=-1) / Rate(K=1) = 10 at y=0 and Ptmin(photon) > 20 GeV/c
" / " = 100 " " " > 100 GeV/c

Main background from $\bar{q}q'$->Wg and qg->Wq' is about x10000 greater at y=0 for K=1 (Standard Model). To discriminate against these as well as multiple interactions backgrounds and rate biases from strong dependence on Ptmin(photon), we need a very fast calorimeter with excellent energy resolution and segmentation.

Rotating in Θ the detector from 70° to 110° and taking data at several angles could optimize our sensitivity to the angular dependence of the W+photon production.

This measurement may become marginally possible soon with the "upgraded" UA1 and D0 (TeV-I, Ref.54) detectors. There, special attention is devoted to excellent hadron resolution using Uranium-LAr calorimetry, which might enable efficient W-mass reconstruction from its W→ 2jets decay, thus producing a statistically significant data sample.

The detection of these rather isolated photons is a classic example where our extremely fast, highly segmented and large acceptance EM Calorimeter could attempt to take clean data near L=10**34 for high statistics. Both experiments would require a fast dE/dx-Charge (C) trigger (1st Level), an

electromagnetic Pt (Pt(EM)) and a combined $\bar{C}$*Pt(EM)*Pt(Jet) trigger (2nd-3rd Level).

4. BOTTOM QUARK PHYSICS:

The large production rate and relatively long life time (1psec) of B-mesons could allow some very interesting topics to be studied:

a) CP Violation Effects, calculated for $\bar{B}B$ production, seem to be measurable in reactions where both B-decays are detected, with one B->l+Y and the other decaying to channels where all decay products can be measured and complete reconstruction of final state is possible,

$$Bd \to \psi\,(l^+l^-) + Ks(\pi^+\pi^-), \quad \bar{D} + D + Ks + \pi\text{'s}, \quad Ks + \pi\text{'s}$$

$$Bs \to \psi\,(l^+l^-) + \phi\,(K^+K^-), \quad \psi\,(l^+l^-) + \bar{K} + K, \quad \psi\,(l^+l^-) + \bar{F} + F$$

For example $Bd \to \psi(ll)+Ks(\pi^+\pi^-)$ is a low efficiency, low rate process and requires secondary vertex (S.V.), lepton and hadron identification down to very low energies (2-3 GeV) with excellent energy and S.V. resolutions. Efficient triggering should involve a lepton trigger (2nd Level), a S.V. trigger (3rd Level) and/or a crude calorimetric or muonic $\psi \to l^+l^-$ trigger, based on the ψ invariant mass. Also, channel $Bs \to \psi + \phi$ should be easier to measure since $\phi \to K^+K^-$ [BR~50%], if π/K I.D. is available.

In Ref.6 they estimate detecting 1300 ψ +Ks events [BR~10**-3]. for Ltot=10**39 (L=10**32) in their central detector ($D\phi = 360^\circ$, Dy= +-1.5). This may be overly optimistic since a more careful estimate gives a BR~ 3*10**-4 (Ref.15). $\bar{B}B$'s are centrally produced with an <Pt>= 6 GeV/c and mostly back to back. So we need 2 opposite arms to see both efficiently: about 500 events for Ltot=10**39/cm**2.

b) Rare Decays: $B \to K^+l^+l^-$ (~10**-5), $\tau + \bar{\tau}$ (~3*10**-6) and Forbidden Decays in the Standard Model (S.M.):

$$B \to \mu + e, \quad \mu + \tau, \quad \pi + \mu + e, \quad \pi + \mu + \tau, \quad K + \mu + e, \quad K + \mu + \tau$$

A BR limit of 10**-7 to 10**-8 seems manageable in Ref.6 with Ltot=10**39, depending on whether both or only one B-decay from $\bar{B}B$ production need be detected. In our spectrometer this could correspond to about 10**-6 to 5*10**-8.

To do the CP violation measurements well, we believe one needs the higher luminosity of 10**33 (vs. 10**32), better detection efficiencies and measurements in several different channels. The last one is all-important for higher statistics and for cross checks on systematic biases (Ref.15). We can compare our ability to study this physics with that of Ref.4 & 6. Their acceptance is larger by x2.5 but they have no π/K/p identification whose significance they may have overlooked. Instead, we insist on π/K/p I.D. at

all energies and emphasize calorimetric and muonic lepton and invariant mass triggers.

We emphasize the prime importance here of our EM calorimeter's extreme speed and excellent sensitivity and resolution down to less than 1 GeV. For microvertex we advocate CCD's for good pattern recognition for hundreds of tracks, which we feel is the cardinal problem at 10**33. Such a detector may then allow us to identify $B\bar{B}$ decays more clearly and in many channels (ψKs, $\bar{D}$DKs, $\psi\phi$, $\psi\bar{K}K$, $\psi\bar{F}F$, etc), instead of just one and at luminosities near 10**33. This could result in x10 to 30 more statistics than in Ref.6, depending on the particular process.

5. τ -LEPTON PHYSICS:

Identification of τ-leptons, even though very difficult, would be extremely important for several studies,

a) Heavy quark flavor cascades like: $t \longrightarrow b+\tau+\nu$
b) New generations of right handed $Z(R) \longrightarrow \tau+\bar{\tau}$, $W(R) \longrightarrow \tau+N$(new neutrino)
c) Search for Horizontal bosons ($\bar{u}c \longrightarrow \mu+e$, $\tau+e$, $\tau+\mu$).

It might be possible to identify τ by its hadronic decays (Ref.17):

$$\tau \dashrightarrow \rho+\nu \ [BR=22\%], \quad \pi+\nu \ [11\%], \quad \pi+\rho+\nu \ [5\%]$$

Since the τ-decay mechanism goes through emission of a virtual W(L;81) which has V-A couplings to quarks and leptons, its polarization could be deduced from the energy distribution of its observable decay products (ρ, π, $\pi+\rho$,etc.) since ν is always left-handed, as shown in Fig.7a (Ref.16).

This simple observation, made at the 1984 Snowmass SSC Workshop (Ref.16), has important implications on the utility of the τ signal as a window to new physics beyond the Standard Model. For example, in a new $W \rightarrow \tau+N$ decay the τ is either purely left-handed or right-handed depending on the nature of the NWτ vertex: the distributions of the τ-decay products signal its polarization which in turn gives information about the parent's polarization W(R) which would distinguish it from a Standard W(L)!

Since the τ mass would be so much smaller than the parent decay mass or Pt in all 3 physics processes mentioned above, its $\rho^{\pm}$ decay product would also be quite energetic, as well as the decay products of the $\rho^{\pm}$,

$$\rho^{\pm} \dashrightarrow \pi^{\pm}+\pi^{0} \dashrightarrow \pi^{\pm}+\gamma+\gamma$$

or

$$\pi^{\pm}+\rho^{0} \dashrightarrow \pi^{\pm}+\pi^{+}+\pi^{-}$$

and in addition the opening angles between the 3 final decay products would also be small and relatively easy to correlate in the calorimeter. In addition, since the ν from τ is always left-handed, the π or ρ or $\pi+\rho^{0}$ product of the τ coming from a W(R) decay would go forward with respect to ν, whereas in W(L) decay backwards (Fig.7a). Experimentally this means that

the observed Pt spectra of these hadrons would be harder in W(R) than in W(L) decays, Fig.7b (Ref.17), which is advantageous in terms of acceptance and pattern recognition in our spectrometer (lucky coincidence!)

Finally, for τ- decays with 2 or more charged tracks, the τ secondary vertex measurement becomes possible and makes the τ signature more unique and easier to discriminate from backgrounds. Also with a lifetime of 0.4 picoseconds (psec) a 1 TeV τ will travel for 7 cm before it decays.

We claim therefore that the τ measurement through its ρ and $\rho + \pi$ decays might not be beyond reach after all. Experience gained by measuring $W(81) \rightarrow \tau + \nu$ and $Z(93) \rightarrow \tau + \bar{\tau}$ at CERN ($S\bar{p}pS$) and FNAL (TeV-I) will be important. However, this would require excellent particle identification information as well as an EM calorimeter with excellent granularity and low-energy sensitivity and resolution, which at the same time is extremely fast (to quickly get rid of multiple interactions background) and far away from the interaction point.

A τ-trigger based on a secondary vertex identification and an isolated $\rho(0+-)$ in the calorimeter seems to be next to impossible, but if possible at all, it would be a decisive tool for very interesting physics.

6. SEARCH FOR HEAVY STABLE PARTICLES:

The kinematics and measurement errors for such objects have been studied at Snowmass (Ref.7 & 18). We find that in our detector both TOF and momentum determination errors are generally important for a mass measurement:

$$m = P/\beta\gamma \; ; \qquad dm/m = dP/P \; + \; (1 + (P/m))^{2} * dt/t$$

Assuming dt = 50 psec and dP/P = 2.5*P*10**(-5) (see later) we obtain contributions to the dm/m given in Fig.8 as a function of m for P/m= 0.1, 1 and 10. We conclude that for "low" mass (.1-.2 TeV) relativistic particles timing errors dominate and for high mass non-relativistic objects momentum errors are the limit.

Their tracking has a characteristic time signature, if they are charged, and a characteristic "minimal" ionization signature inside a calorimeter. Their energy deposition signature in a calorimeter would be very small and they could be overwhelmed by low-Et debris.

It requires precise tracking, long lever arm, strong magnetic field, precise timing and finally fast calorimetry with high tracking ability and excellent sensitivity to minimum ionizing tracks, in environments with luminosities of 10**33/cm**2/sec or higher.

Triggering requirements would include a high-Pt calorimetric trigger and a μ-like one. Perhaps, it might be also possible to use a precise multiple timing trigger based on calorimetric and μ detector information.

Scanning at several different polar angles with the Jet Spectrometer (Fig.15) or at polar angle correlations in combination with a second "minor arm" (Fig.16), is tantamount to searching in a large fraction of the phase space available for such particle production.

7. QUARK-GLUON PLASMA SEARCH/STUDY:

Finally, existence of QGP would signal a new state of matter and thus most interesting and worth studying at SSC. In Appendix 2 we discuss some theoretical ideas relevant to QGP.

Experimentally, a flattening out <Pt> distribution for dNc/dy >8 in the UA1 data (Fig.2) might be a signal that a phase transition may just be starting. JACEE, a cosmic ray collaboration, starts where UA1 stops by observing a flat Pt distribution at low energy densities, $\mathcal{E}$, as shown in Fig.11 (Ref.21), which however takes off abruptly, when $\mathcal{E}$ >2.5. This could be consistent with a phase transition, around $\mathcal{E}$ = 2.5-3.0 GeV/fm**3, leading to the ignition of a QGP. It is not yet clear whether at TeV I (2 TeV) one can "pump" enough matter out of the vacuum to definitely initiate a QGP and not just start a phase transition, which after all might not be easily observable or even necessary to exist at all for a plasma to start.

A QGP would not simply produce a high multiplicity particle ensemble with a low-Pt spectrum, but a rich array of particle types, conveying several kinds of information. One could devise a set of plasma diagnostics to follow and study its creation and evolution, using this information:

1) Measure very high multiplicities dN/dy= 10-100 or even higher. This gives the entropy density at the cool-off temperature and its upper limit when the plasma was initiated, since according to Boltzmann entropy never decreases in a closed system, or gives information on the phase transition characteristics, if the plasma state is not reached.

2) Measure the mass and/or Pt spectrum distributions of dileptons and direct photons from very low (100MeV) to high energies. These could be produced in excess, since they could come freely out from inside the whole plasma volume (Ref.26), from preignition to cool off, and trace its energy density and temperature evolution.

3) Detect quark jets of high Pt, possibly evaporated from the hot plasma surface at an early stage, in association with the rest of the plasma (Ref.27). In principle, from their rate we could measure the plasma radius, since

$$\text{Rate(jet)} \sim \text{Area(surface)} / \text{Volume} \sim 1 / \text{Radius(plasma)}$$

From their Pt spectrum we measure its temperature and from the Rate vs Pt correlation the Radius vs Temperature relationship for the plasma. It would be extremely interesting if an actual calculation showed that in fact such a relation first exists and second the effect is not masked by background processes.

4) Identify heavy flavors in the final state at all energies. Measuring an excess could mean existence of plasma non-equilibrium for reactions like gg -> $\bar{c}c$ due to the finite time of plasma expansion: not enough time for small initial concentrations of heavy quarks to reach dynamic equilibrium (Ref.27). In principle, with such non-equilibrium measurements one could estimate plasma expansion times and/or initial quark flavor and gluon concentrations.

5) The velocities of constituents inside the plasma are the same on each outgoing plasma wave-front, but the momenta (P) are proportional to the individual constituent masses: the heavier the quark the harder its P-spectrum will be (Ref.53). In other words, a hydrodynamically expanding plasma should behave like a new type of a mass spectrometer, by magnifying the separation between the momentum spectra of different quark masses. In effect it gives a boost to the heavy quark rates vs Pt, as compared to the lighter ones.

These and other types of measurements impose a series of formidable detector requirements among which the most demanding one is the precise measurement of low to high-Pt jets in the midst of a low-Pt, high multiplicity plasma final state.

They require fast, dense and highly segmented calorimetry as well as good energy sensitivity and resolution down to the very low energies of 100 MeV to safely remove multiple interactions, measure multiplicities, identify hadron flavors and photons and finally accurately measure photon, lepton and hadron energy distributions. The QGP central production kinematics could be well matched with the detector at a nominal position of y=0. Triggers which would enhance the QGP signature could include:
a) charge multiplicity trigger (and approximate π^o or photon multiplicity trigger ?) and
b) a large calorimetric energies ratio

E-M shower energy / Hadron shower energy

Minimizing background from other sources, like showers in magnet poles before apparatus, is important for clean measurements.

IV. EVALUATION OF DETECTOR REQUIREMENTS

1. PHYSICS REQUIREMENTS

Almost all the physics topics examined above involve detection of jets, with the QGP and the Jet studies the most demanding ones. To properly study this physics at L= 10**33/cm**2/sec, one has to satisfy the following basic requirements in a large acceptance specialized device:

i) Fast calorimetry and fast enough or smart enough jet triggers to handle a background at a rate of $dEt/dt/d\Omega$ >160 GeV/μsec/str. Use fast calorimetry with readout gates less than 50 nsec.
ii) Calorimetry with the best possible energy resolution for jets. Use calorimeter with good sensitivity and uniform response to both EM and hadronic showers from 1 GeV to several TeV.
iii) EM calorimetry with the highest possible density and segmentation and TOF capability to resolve photon/π^0, $e/\pi^0+\pi^\pm$ from .2 GeV to 5 TeV, as well as remove background from multiple interactions. Use a "continuous medium" EM calorimeter of high density (> 5g/cm**3).
iv) EM calorimetry with energy resolution better than 5% for electrons and photons below 5 GeV. Use a "continuous medium" EM calorimeter.
v) Vertex detectors that can provide efficient secondary vertex triggers and with excellent double track and pattern recognition capabilities. Use CCD's.
vi) Excellent TOF, dE/dx and tracking resolution for new heavy particle and low energy particle identification. Use BaF2 and Drift Chambers (D.C.).
vii) Particle Identification (π/K/p) from 15 GeV up to the highest possible energies. Use dE/dx and a gas RICH detector.
viii) Excellent electron and μ identification. Use TRD, calorimetry and μ-toroids.

These physics requirements have motivated us to come up with several ideas and solutions which form the basis of our detector design. We discuss them below in detail.

2. VERTEX IDENTIFICATION

Concerning all detectors in general and this one in particular, the SSC environment is peculiar in 2 quite opposing ways:

a) There are about 400 tracks from minimum bias events to sort out. In addition, in several physics processes of interest one ends up with more than one secondary vertices per event, like in

$$t \rightarrow b + \tau + \nu\,, \qquad B \rightarrow \tau + \bar{\tau}\,, \qquad W \rightarrow t + \bar{b} \rightarrow t + (\bar{c}+\mu+\nu)$$

to be distinguished from the main vertices of 100 or so background events in 1μsec. If much is to be gained in such cases, it will have to come from vertex reconstruction in 2-dim (on the transverse plane) and if possible in 3 dimensions.

b) The large multiplicity, per event and per high Pt jet in general and of B-decays in particular, could provide a high enough number of tracks to suggest the 3-d vertex reconstruction as a viable possibility. It has already been demonstrated in Ref.31 that using all charged tracks, instead of only leptons, enhances sensitivity of the impact parameter distribution to B-lifetime. Also, the $\langle Pt \rangle$ would be higher at SSC for many processes and so decay distances would be longer. With 3-d reconstruction one can take full advantage of this to separate the primary from secondary vertices.

However, an event by event 3-d reconstruction is a complicated pattern recognition problem compared to the straightforward impact parameter distribution technique, but the resolution improvement would be substantial. These considerations force upon us the CCD as probably the only promising solution. A CCD with its true 2-dim segmentation provides unambiguous points in 3-d space, which gives it a decisive edge in 3 well defined aspects:

a) The higher multiplicities per event and the minimum bias background, superimposed on it, make double track resolution the most serious consideration for microvertex detectors. The CCD is far superior than strips or fibers in this respect.

b) It could handle the severe pattern recognition requirements imposed by the very high multiplicities and several vertices per event and

c) The triggering requirements upon a microvertex at SSC are severe. This so far has proved to be a futile exercise with silicon strips. It will be easier for CCD's.

3. PARTICLE TRACKING

In the tracking system design, we emphasize 2 characteristics as highly desirable:

1) High Position Resolution per track at each station by taking a large number of measurements at each station, along with high precision surveying of each chamber down to 20-30 μm. Then a 150μm resolution per channel, for example at the 4th station, gives about 40μm per station per track.

2) Provide many true space-time points for each track: Wire planes should be exactly staggered in pairs by half cell (Ref.50 & 51). In addition, charge division on each wire and a plane of strips between the planes of each pair should be considered. The staggering has 2 important properties:

a) The sum of the 2 arrival times at the wires of each pair (t1,t2) is independent of the track position and gives the true time, t, of the particle's passage thru the chamber, with an error dt $\sim$ 2 nsec, apart from an additive constant D, the chamber half width.

b) Excellent double track resolution, at least in principle, since

$$t1 + t2 = t + D - d12$$

where d12 is the distance between the two close-by tracks

$$d(d12) = d(t1+t2) * v(e) = dt * v(e) = 200\ \mu m\ /\ \text{wire-pair}$$

where $v(e) = 100\ \mu m/nsec$ (: a fast gas)

The resolution with this new technique would be an order of magnitude better than that obtained by the standard technique of pulse to pulse discrimination used so far.

4. ENERGY RESOLUTION: GRADING WITH DEPTH

An important physics requirement and one of our prime design goals is excellent EM energy resolution over a large dynamic range from 0.1 GeV, e.g. photons in QGP studies, to 10 TeV, e.g. direct photons from composite quarks. Both measurements probe extremely interesting phenomena. This is possible only with "continuous media" calorimeters (NaI, BGO, BaF2, SCG1-C, SF5, etc.).

BaF2, our present choice, could satisfy the energy resolution, speed and density requirements for the EM calorimeter. From its two scintillation light components, the one of interest to us is the extremely fast one, shown in Fig.13 (Ref.35), with less than 1nsec decay constant, a UV-spectrum of 160-250 nm and a yield of 2000 photons/MeV. It will require an R&D effort to try to isolate it from the other much slower component (1μsec).

Then a standard thin vacuum photodiode (Ref.36 & 37) with gain=1 could deliver N(pe)= 500 pe/MeV, which corresponds to a photoelectron statistics error of $1.4\text{x}10^{**}\text{-}3/\sqrt{E}$. This is at least an order of magnitude better than the $1.5\%/\sqrt{E}$ obtainable with the best practical EM calorimeters ever built.

A preamplifier with JFET input transistors (Ref.38) with a t(r)= 5nsec (risetime), connected to a 3cmx3cm area photodiode, could exibit an RMS noise as low as 3000 electrons, which corresponds to a .6% per channel error at 1 GeV and does not really limit the best EM resolution we can expect in practice from such a detector. Therefore the (BaF2, Photodiode, Preamplifier) EM calorimeter system is a rather well matched one. Table II shows these errors.

With SCG1-C scintillating glass we have actually measured a yield of 15 pe/MeV using such diodes (Ref.14). A heavier glass type under R&D now having the same light output (Ref.39), with a t(r)= 20 nsec risetime preamp could give an RMS error of about 10-15% per channel at 1 GeV. If the shower energy of a 1 GeV electron is collected by several segments, the resulting resolution could be 50% or worse. If we insist on excellent low energy resolution, this is clearly inadequate for EM. However it is equivalent to the best expected from a practical hadronic calorimeter of $40\%/\sqrt{E}$. Therefore the (Scint.Glass, Photodiode, Preamplifier) hadron calorimeter system is a well matched one.

In effect, the electronics noise worsens with depth but in step with the inherent energy resolution of the calorimeter and thus does not dominate the overall resolution.

Finally, the important problem of equalizing the calorimetric response for electrons and hadrons must be solved. In the past we have proposed a solution for scint.glass (Ref.40) where the separate measurements of its Cherenkov and scintillation light components are used to estimate the EM fraction of energy in a hadronic shower. For the present scheme, R&D on BaF2 and scint.glass as well as calorimeter prototype beam tests would be necessary.

5. OPERATIONAL SURVIVAL

The detector must be able to comfortably survive the radiation levels of the 10**33/cm**2/sec luninosity. In addition the calorimeter of a jet spectrometer at y=0 is a prime example of a candidate to attempt to run at an even higher luminosity up to 10**34.

The highly resistant to radiation damage BaF2 (EM) and heavy scint.glass (hadronic) around 90 and at 7m away from the beam would be able to survive at such luminosities (Ref.41) for several years, something we take full advantage of: our design matches perfectly the capabilities of this fast "continuous media" calorimetry to the physics requirements for excellent energy resolution and high luminosities.

The detector must have large enough acceptance to do the physics and still be able to stand the high multiplicities; an estimated number of about 250 particles and close to 200 GeV of energy deposited in 1 str per μsec. One could raise the trigger energy thresholds with obvious penalties among other things on the overall detection sensitivity and energy and position resolutions. This along with the use of a U-LAr calorimeter is the standard strategy advocated so far for a general purpose 4π detector.

Here we advocate a totally new strategy based on a combination of timing and segmentation that leads to the top performance asserted for this detector and in the most efficient manner:

6. TIMING STRATEGY: SPEED GRADING WITH DEPTH

It is based on the simple observation that the high rate backgrounds, min.bias and low-Pt jet events, essentially consist of many low energy particles, of less than 2 GeV each around 90°, with their calorimeter penetrating little energies attenuated very rapidly as a function of depth: About 40% of all the energy, in the form of π^0 EM showers, will be deposited in the first 20-25 L(rl), anyway. For the hadrons carrying the 60%, the softer their energy spectrum the higher their rate is, but they also penetrate less into the calorimeter. At the end, about 75% of the total energy is deposited in the first 1.5 L(al), 25% in the next 5.5 L(al) and

only a negligible amount of less than 1% is deposited at depths beyond 7 L(al).

Our strategy then consists of grading the calorimeter speed vs depth: we design it to slow down with increasing depth! Then, the calorimeter has a relatively uniform response to min.bias background with all parts seeing comparable amounts. This allows for optimized background sharing giving the best possible performance at the minimum cost and effort. This is seen better in Table III, where all the calorimeter types with their trigger gates, and actual energy collected in GeV for the background are shown as well as the background to signal ratio for 1, 10 and 100 GeV energy electrons, π's and jets.

Emphasizing fast calorimetry is in the right direction, as far as increasing background rates are concerned, but it also gives us, for free, TOF capability for particle identification up to roughly 4-5 GeV for π/K separation. This becomes possible also because of the large distance of the calorimeter from the event vertex.

7. SPACE-TIME SEGMENTATION

Next we consider the combination of the extreme readout speed, 100MHz, of the EM calorimetry with its excellent tower segmentation, Dy=.004 and $D\phi$ = 4.3 mrad, for what amounts to a superfine space-time segmentation, an idea we have already investigated at an LBL Workshop for future colliders (Ref.37). With an average of 2 particles/10nsec in the central calorimeter, Dy=$D\phi$ =+-.5, shared by 40k EM towers of 3x3 cm**2 cross section, we estimate an average of 5*10**-5 particle hits per tower per min.bias event at L=10**33. This allows an excellent background rejection capability all the way up to L= 10**34, without resorting at all to Pt thresholds.

8. CALORIMETRIC SPACIAL RESOLUTION

We most emphasize this detector feature to resolve high energy direct photons from π^0 and electrons near jet cores, most critical for the success of our prime physics goals, including QGP studies with extremely high multiplicities. It is not clear at what energy one stops resolving single photons from π^0. We make the following 4 observations relating to this problem and its solution in our detector scheme:

a) Whereas the 2-photon distance, 2mm at E(π^0)= 1TeV, decreases linearly with the inverse of the photon energy, the shower's transverse size decreases and the longitudinal profile increases logarithmically with energy. The fine 3-d EM calorimeter segmentation and hence detailed partition of shower depositions would permit accurate calculations of shower position and width (1st and 2nd moments) and shape (higher moments) in 3 dimensions.

b) The 2-shower separation resolution is highest at the beginning of the shower evolution. This problem has a striking similarity with the double

track resolution problem we encountered earlier with the drift chambers and proposed to solve using the staggered cell topology. Since drift chamber rates are manageably low at 7m from the event vertex, we can attempt using the same technique for EM showers, with chambers at 2 different depths inside the EM calorimeter at a few L(rl) from the front.

c) The photon conversion probability or starting point depends on the number of photons. To maximize the starting point detection sensitivity one could distribute longitudinally the first 0.5 L(rl) as much as possible but in a controllable manner. This would be partly accomplished automatically in our design by the devices before the EM calorimeter, comprising about .15 L(rl). Another .2-.3 L(rl) of preconverter could be distributed between the last few drift chamber planes right in front of the EM calorimeter. Our detector design, based on these principles and especially on (b), would be rather unique in discriminating high energy photons/π^0 at least up to 1-2 TeV.

d) Finally, the higher the calorimeter density the better the 2-shower resolution can be. If thin photomultipliers of a few dynodes with a gain of x100 or higher for example were available, scint.glass would be the right choice for the EM calorimeter also, rather than BaF2: the preamplifier noise would not be limiting the resolution of electrons/photons with energies 0.1 to 2 GeV. As a byproduct, EM calorimeter density would be 1.5-2.0 times greater than that of BaF2. Having only scint.glass, for both EM and Hadron calorimeters, would represent an important simplification and improvement at the same time. In addition it would probably result in big money savings by eliminating the BaF2 cost.

The calorimetric energy, magnetic momentum, microvertex, drift chamber, RICH, TRD and dE/dx along with the transverse and longitudinal shower information would be used to resolve electrons from $\pi^{\pm}$'s, $\pi^0+\pi^{\pm}$ overlaps and early photon conversions in the detector.

V. DETECTOR CONFIGURATIONS AND PARAMETERS

1. DETECTOR CONFIGURATIONS

The "Jet Spectrometer" main arm, as shown in Fig.14, consists of
1) a CCD microvertex detector,
2) a DC Tracking and dE/dx system,
3) a magnetic spectrometer,
4) a gas Cherenkov ring imaging counter (RICH),
5) a dE/dx system of counter hodoscopes, after RICH
6) a transition radiation detector (TRD),
7) EM Calorimeters,
8) Hadron Calorimeters,
9) Muon Toroids and
10) a time of flight (TOF) system.

The front face of the EM calorimeter at a distance of 7m from the interaction diamond, would have an aperture of about 3 str and in its nominal position it would be centered around θ = 90° (y=0), with respect to the beam direction, and would cover 1/4 of the full azimuth:

$$D\phi = 90°, \qquad -0.9 < y < 0.9 \qquad (\text{Jet Spectrometer})$$

The second arm could have a much smaller calorimeter ("Minor Arm") and at the same time a larger angular coverage

$$D\phi = 120°, \qquad -1.5 < y < 1.5 \qquad (\text{Minor Arm})$$

if the calorimeter starts at 1.5 meters, as shown in the schematic of Fig.15. It would probably cost about 5% that of the "Jet Spectrometer" to build. Its main limitations relative to the Jet Spectrometer would be:
a) No single photon identification (I.D.) above 30-40 GeV.
b) No good electron I.D. near narrow jet cores.
c) No hadron I.D. above 30 GeV.
d) Good performance would be limited below 5*10**32. Only energy flow could be measured near 10**34.

For single photon studies, like W+photon, we visualize a θ -rotation for one or both arms around y=0. At the same time the total spectrometer length, and the calorimeter distance from the event vertex, should change accordingly (Fig.15) so as to maintain cell occupancy probabilities, TOF and momentum resolution and radiation damage at comparable levels at all angles. This is the first time consideration is given for an SSC detector with scanning capabilities. This technique may be of general utility for many different physics studies.

If azimuthal acceptance proves to be limited for bottom physics or QGP studies, one or both arms could be moved at half of their nominal distances, for a close to 2π azimuthal coverage (Fig.16), compromising somewhat some measurement capabilities. If one or more resolving capabilities are inadequate above certain energy, like photon/π^0, electron/jet-core, TOF, RICH, or overly compromised at luminosities near 10**34, one or both arms could be moved to a longer distance from the event vertex (Fig.16), at a loss of rates and acceptance. That's partly why we have designed its nominal acceptance to be much higher than 1 str. In the following we describe each detector component in more detail.

2. SECONDARY VERTEX DETECTOR

A typical CCD design would consist of 6 CCD planes necessary for efficient tracking and triggering (300μm*6=1.5% L(rl) : seems OK). Table IV gives basic parameters of such a system.

In most of the physics discussed above, secondary vertex identification and precise tracking play a prominent role. The main purpose of the vertex detector is to search for secondary vertices. It also assists the drift chambers for the track reconstruction in front of the magnet.

Silicon will survive several years of running at L=10**33/cm**2/sec. There are problems, however: Present day electronics will have to be improved by at least one order of magnitude to be able to withstand the above luminosity. Finally, one must solve the slow speed problem of the CCD readout system. Parallel readout R&D is necessary to make CCD's usable.

Specifically for a jet spectrometer, the capabilities of a CCD microvertex detector are particularly enhanced for several reasons:

a) Much less amount of data has to be handled and easy routing of readout cables is possible compared to a 4π coverage. Frequent access and servicing are also easy, whereas in 4π almost impossible.

b) Except for the first one, moving the CCD planes far from origin (10-15cm) becomes feasible because the 5 times longer lever arm (7m) results in the same resolution as with 4π detectors with 1.5m radius and 1.5-2cm of MVD from beam line (linearly). Also, the better the D.C. accuracy the farther the MVD could go (linearly). This results in large transverse separations between tracks, low occupancy levels per cell and 25 times less radiation damage.

c) Existence of precise space-points from D.C.'s quickly allows good primary vertex z-determination and connection of interesting tracks from outer detector to CCD hits. This particular DC+CCD coordination may be the key to providing a feasible secondary vertex trigger at the 3rd level at L=10**33.

3. DRIFT CHAMBERS

Four stations of drift chambers are employed. Their locations are shown in Fig.14 and their parameters are listed in Table V. The total number of readout channels(wires and strips) is 120*10**3. These chambers offer here some unusual capabilities:

a) Excellent momentum resolution for charged tracks at all energies up to a few TeV/c.
b) The only energy measurements for tracks escaping the calorimeter, therefore measuring in detail the tails of a jet.
c) Excellent rejection of background events using the timing of each chamber pair.
d) Aid the TOF measurements in resolving double hits and other systematic biases.
e) Because of their long lever arm, their high resolution allows most of the CCD's to be far away from the beams and still preserve their high vertex precision and, most important,
f) very quickly could form tracks of interesting events providing the primary vertex z measurement, impact parameters and connecting points to the CCD system, all vital information needed by the CCD's to form secondary vertex triggers at the 3rd Level.

4. MAGNETIC SPECTROMETER

Magnetic bending could be provided by a solenoidal-like superconducting magnet surrounding the beams, as shown in Fig.14

Radius = 1.3 m

and

B = 1 Tesla

bending cylindrically (essentially vertically at the Spectrometer). It would have two arms, left and right of the interaction point, leaving an open space of 1.8 m for the interaction products to enter freely the outer part of the detector.

Assuming a total drift chamber resolution, for the last station, of $\sim$ 40 μm, by grouping together several plane measurements, we can achieve a momentum resolution of DP/P= 2.5*10E-5 * P(GeV/c). At 1 TeV/c this is 2.5%. This kind of precision is basically due to the long lever arm (x20, compared to a 1.5 m radius detector) and the excellent track resolution (x5 to 10, compared to resolutions available in current detectors).

A dipole or any other kind of massive magnet is avoided and a minimum of mass is kept near the beams in the Spectrometer proximity to

a) avoid shower backgrounds into the calorimeter; mainly for QGP, weak physics (CP-violation,etc), studies of jets and physics at L=10**34,
b) minimize backgrounds in the D.C.'s, RICH and TRD, especially bothersome to fast trigger generators using D.C. and EM calorimetry information.

Vertical bending is to be preferred:

a) Decoupling of the momentum measurements from vertex z measurements. Little Pt distortion on each event as a whole and in particular on each charged track, which is very valuable for fast and accurate calorimetric Pt triggers, at the 1st Level.
b) Easy and accurate z and momentum measurements for each event's primary vertex. Especially for L=10**34, distant drift chambers might suffice.

5. LOW ENERGY PARTICLE IDENTIFICATION : TIME OF FLIGHT (TOF)

High precision timing would enable particle identification up to a few GeV, identification of new heavy stable particles, and improve rejection of backgrounds from multiple interactions.

The D.C. timing information of 1-2 nsec/wire-pair from 80 such pair measurements is valuable in tracing in time each particle for background rejection purposes.

The BaF2 EM towers, however, will provide the most precise timing. From a 1 GeV shower deposition, in a small 3x3 cm**2 by 3 L(rl) long block, 500k

photoelectrons could be collected in less than 1 nsec. This, in principle, corresponds to a time error of less than 1 psec. Some electronics R&D and Monte Carlo studies would be important here to find just how low the actual limit of this technique might be. In practice, however, more like 50 psec may be the limit at the present time, restricting the π/K separation at low energies up to 4-5 GeV. This matches perfectly with the dE/dx particle identification capability, starting to be unambiguous above 4 GeV/c, as shown in Fig.17 (Ref.42).

Finally, another valuable aspect of our TOF scheme is that it ties precisely in time the particle identification with its calorimetric energy deposition, guarding against multiple interactions background.

6. MEDIUM ENERGY PARTICLE IDENTIFICATION : CHARGE IONIZATION (dE/dx)

The analog information of 120 drift chamber planes per track with 1 cm sampling length and Xe-gas at 1 atm could allow π/K/p identification between 4 and 80 GeV/c. An accuracy of 3% has been obtained with Ar-gas, in the EPI device (CERN), corresponding to a 3 std π/K separation at 70 GeV/c (Ref.43).

For tracks that bend out of calorimeter acceptance, less precise TOF and RICH information is available and they traverse a smaller number of planes, but we should still manage to identify them: the lower their momentum the lesser the number of dE/dx samples we need for particle identification at medium energies and below 2 GeV/c the combination of drift chamber TOF and dE/dx might be adequate.

At low luminosities, the medium energy particles could also be identified with a liquid RICH counter and D.C. dE/dx information without much need for super precise TOF. However, near L= 10**33/cm**2/sec or higher, not much else will survive and BaF2-TOF will probably become critically important as the only technique left: High particle fluxes (see Table V) will produce positive ion space charge effects, which will totally wipe out all dE/dx precision information (Ref.42), with 800 kHz singles rates per wire at the last station of D.C.'s (magnet off) at 10**34.

7. HIGH ENERGY PARTICLE IDENTIFICATION : RING IMAGING CHERENKOV (RICH)

Assuming that the resolution limit to the Cherenkov angle determination is the chromatic abberations, He-gas is the best for our configuration, but the photoelectron statistics would be dangerously low, so a 5% fraction of CF4 is added. That may allow us to separate π/K up to 400 GeV/c (Ref.56).

The ring imaging Cherenkov counter covers the central +-0.5rads of the spectrometer. The parameters of the radiator and the photon detector are listed in Table VI. The mirror is split into two pieces (Fig.14). Each piece is tilted around an horizontal axis parallel to the beams, so that they reflect and focus the photons outside the spectrometer acceptance into the photon detectors placed up and down of the horizontal plane containing the beams.

Because the π threshold is $\sim$15 GeV, the photon detector rate will be much lower than the charged particle rate inside the radiator (see Table VI). The ISAJET (Ref.44) Monte Carlo predicts that, for min.bias events, the rate for $\pi^{\pm}$'s with momenta above 10 GeV is less by three orders of magnitude than the total $\pi^{\pm}$ rate. This means that the photon detector rate will be much less than 10**5 Hz for L= 10**33.

Furthermore, each photon detector, of 60cmx100cmx3cm dimensions, could be oriented so that it lies in a ϕ =constant plane and thus intercepts a negligible fraction of 2π in azimuth, Dϕ =10mrad and a y-interval of Dy=+-.16, corresponding to 0.4 min.bias charged tracks per 1 μsec.

8. ELECTRON IDENTIFICATION : TRANSITION RADIATION DETECTOR (TRD)

The TRD detector is located between the RICH and the Calorimeter, at a distance of about 6m from the beams, is about 1m long and covers only the central spectrometer region, (Dϕ =0.8)x(Dy=1.0). Its parameters are given in Table VII. Experiment E715 at FNAL (Ref.45) used a TRD stack of 12 PWC stations, with 70%Xe+30%CH4, each having 210 layers of 17 μm polypropylene (CH2), with a total thickness of 10% L(rl). Using the cluster counting technique in the momentum range of 10-100 GeV and requiring N(active stations) >7 and N(clusters) >14, they obtained a π/e rejection of 1500.

Here, the range of energies of interesting electrons is greater and it becomes harder to discriminate them from π's. Fig.18 shows the number of photons for E715 modules vs. γ = E/m, the Lorentz factor. However, our calorimetric π/e separation, close to 1000, would be more than a factor of x10 greater than that of the E715 calorimeter and would be the only technique ultimately left for energies > 200 GeV.

The TRD performance is also complicated by interactions of the traversing particles, which is proportional to the TRD thickness times the particle multiplicity. Here the particle multiplicity is high and thickness must be kept at a minimum to avoid photon conversions too far away before the EM calorimeter. Clearly the optimum thickness would have to be compromised between conflicting measurements. Lacking such a study, we consider using 1600 layers with a 0.06 L(rl) thickness as a reasonable starting guess.

9. CALORIMETRY

Fig.14 shows the calorimeter configuration in the main spectrometer arm and Tables VIII & IX give its various parameters. It is subdivided geometrically into a central calorimeter of

$$|Dy| = |D\phi| < 0.5$$

and a peripheral one of worse granularity, sampling and quality in general, which forms a rectangular ring around the central one of approximate width

$$0.5 < \sqrt{Dy^{**2} + D\phi^{**2}} < 0.9$$

They have similar transverse and longitudinal segmentation and consist of several types of calorimetry. We describe them explicitly for the central region:

A) 20 L(rl) (radiation length) of BaF2 (L(rl)=2.05cm), which is about 1.4 L(al) (nuclear absorption lengths), in a "fly's eye" arrangement of towers with square 3x3 cm**2 transverse cross sections and 5 longitudinal segments each (1+2+4+6+7 L(rl)). Each tower segment is read out with thin photodiodes, sensitive only to UV-light, to pickup the fast scintillation light component of BaF2. This could provide excellent timing accuracy and EM energy resolution DE/E $\sim$1%/$\sqrt{E}$, simultaneously.

B) 5.5 L(al) of scint.glass (one of the new high density types with density $\sim$ 8g/cm3 and L(rl) $\sim$ 1.6 cm) in a tower arrangement with square 10x10 cm**2 tower cross sections and 4 longitudinal segments (1+1+1.5+2 L(al)), each read out again like the BaF2 blocks, but now collecting both the Cherenkov (Tdecay $\sim$ 1nsec) and scintillation UV-light (Tdecay $\sim$ 50nsec). The EM energy resolution for such glasses is about DE/E = 1.5%/$\sqrt{E}$ (Ref.46). The hadron resolution obtainable with BaF2+Scint.Glass combination depends primarily on the ratio of responses to the EM and hadronic parts of a shower. To safely estimate it, we need to build a calorimeter prototype and test it with electrons and π's in a test beam. Right now we can only speculate that DE/E will be better than 50%/$\sqrt{E}$.

C) Leakage Hadronic Calorimeter: 6 L(al) of Pb with a hydrocarbon gas as the sampling medium. Absorber sampling thickness of 4xL(rl) (2.2cm) for the first 3 L(al) and 8xL(rl) (4.5cm) for the rest which plays the role of a leakage section. One can reasonably expect on the basis of DO tests (Ref.29) of Uranium + Liquid Argon, and of L3 tests (Ref.49) of U+gas prototypes, resolutions of the order of 60%/$\sqrt{E}$ for this last calorimeter section. We expect to operate this section with preamplifier integration times of order 100 nsec.

BaF2 and Scint.Glass are used only in the first 7 L(al) of the central calorimeter. Pb+gas is used throughout the rest of the detector. Table II shows preamplifier risetimes, noise and noise/signal estimates using diodes and gas/pad readouts for 1 and 10 GeV electrons and hadrons. In this design the min.bias background energy is distributed as follows:

a) $\sim$74% in the first 1.5 L(al), most of which is the π^0 energy, as BaF2 fast scintillation light, read out with a 10 nsec gate using 100 MHz FADC's.

b) $\sim$25% in the following 5.5 L(al), which contains about half of the hadron's energy, as fast Cherenkov and slower scintillation light (T(decay)=30nsec) from Scint.Glass, within a 50 nsec gate and

c) a negligible leftover of about 1% of energy is collected in a 6 L(al) deep Pb+gas shower leakage section within 200 nsec.

10. MUON IDENTIFICATION

The calorimeter leakage section is followed by 12 Fe-plates, each 1 L(al) thick, with 4 tracking chambers in each gap (2X,2Y) to identify and track muons and non-interacting punch-through. Coils surround the Fe-plates to provide momentum analysis for the penetrating particles and muon and punch-through triggers. Tracking and momentum matching before and after the calorimeter guarantees proper muon or punch-through identification. Subsequently the spectrometer provides the best momentum determination.

VI. TRIGGERING

1. 1-JET RATES

The pp $\rightarrow$ jet+anything production rates and the number of events for one year's (10**7 sec) effective running as a function of the Pt threshold are listed in Table X. These estimates are based on the EHLQ predictions (Ref.47) for a $\sqrt{s}$= 40 TeV energy and a luminosity L= 10**33/cm**2/sec. We have assumed that the jet axis is contained in the central part ($D\phi$ =Dy=+-0.3) of the detector. This assures that at least 85% (98%) of the total energy of jets with <Pt>= 100 GeV (2TeV) respectively will be detected (Ref.48). The number of particles that enter the spectrometer is about 20 (200) for jets with <Pt>= 100 GeV (2TeV) respectively. From Table X we see that an effective trigger rate of a few Hz would require a hardware Pt threshold of about 200 GeV in 1 str, the "standard" jet trigger size (Ref.55).

The obvious background to the jet triggers is from min.bias events during the integration time of the calorimeter. This background was discussed earlier and is shown in Tables I & III with the magnet off. Turning the magnet on may reduce it by$\sim$1/4.

2. JET TRIGGERS

It is already well known how to form a 1 str jet trigger, especially with a calorimeter of fine 3-dim segmentation. This could be done at the 1st Level. We only comment that one could supplement this with additional conditions, dependent upon the specific type of jet one is searching for,

a) a relatively hard core to discriminate from high multiplicity fluctuations of multiple interactions background for jet energies around 10-50 GeV (1st to 2nd Level).

b) a lepton (electron, muon) and/or a microvertex trigger to characterize its flavor cascade (2nd to 3rd Level).. etc.

3. ELECTRON TRIGGERS

An electron trigger was already pointed out by others (Ref.1), based on matching TRD groups of wires and calorimeter towers to be used for electrons at high Pt. An efficient and fast electron trigger would need:

A) High discrimination power from hadrons. This can be based on the difference of its calorimetric EM shower pattern vs. the hadronic one from π's, K's, etc., and/or on transition radiation (TRD). The first one can give more than 1:100 rejection and is preferable for SSC conditions since
i) our EM calorimeter readout can be almost 2 orders of magnitude faster than that of a TRD and therefore can best handle very high event rates;
ii) for high energies > 80 GeV the TRD ability diminishes rapidly, whereas that of the transverse and longitudinal segmentation does not.

This calorimetric part of the trigger is implemented transversely, by forming combinations of 9 EM tower clusters at the 1.5 Level, with the central tower having the highest energy and a relatively small amount of energy in the surrounding 8 towers, and longitudinally, by requiring a small amount of energy in the first 1-2 L(al) of the hadron tower roughly behind the 9 EM ones. The trigger's efficiency remains high throughout the electron energy range down to a few GeV.

B) High discrimination power from $\pi^0 \rightarrow$ 2 photons. This we can do with a requirement for a charged particle (dE/dx) hit, a "charge" trigger, using a scintillation counter hodoscope, in front of the calorimeter. It could consist of 3cmx3cm square blocks in a "fly's eye" arrangement. Read out with photomultipliers would be as fast as BaF2 with 100% efficiency.

The angle between the charged hit and the shower center would be calculated for a 2nd Level trigger with an accuracy better than 1 cm or 1.4 mrad. A Monte Carlo study (Ref.1) has shown that in a 5 TeV jet the fraction of particle pairs with angular separation less than this would be about 1:800.

We feel that these conditions are very powerful, especially because they alleviate the need for slow, complicated and hard to implement DC tracking and TRD requirements. Their implementation, relying heavily on fast calorimetry and fine 3-dim segmentation, could be viewed as a rather unique capability of this detector scheme.

4. DIRECT PHOTON TRIGGERS

By requiring (no charge) instead of (charge), an electron trigger could be converted to a photon one, but much less efficiently unless

a) E(photon) > a few TeV, whereby from kinematics a jet cannot easily contain a π^0 of comparable energy, e.g. it would take on the average a jet energy > 20 TeV to produce a 2 TeV π^0 and only 1/3 of the time. If in addition a 0.1 str jet trigger found little energy around the single photon a π^0 rejection of 100 could result, only from that.

b) E(photon) < 25 GeV, where the 2 photon showers from π^0 would be clearly separable and a quick (2nd Level) pattern recognition would be possible.

The single photon triggering at intermediate energies would require the development of sophisticated 3-dim shower pattern recognition algorithms fast enough to be implemented at the 3rd Level trigger stage.

5. SECONDARY VERTEX TRIGGER

Our objective is to obtain a 3-dim reconstruction of a secondary vertex or its 2-dim. projection on the transverse plane and fast enough so as to be able to use it in a 3rd Level trigger. This automatically implies one must obtain at least 2 vertices, the primary one of the event and a secondary one, and their relative position vector whose length is well above the vertex position errors, unless the transverse beam position is known for each event, within a few μm. We have considered a procedure consisting of the 4 following steps:

a) First, the dE/dx scintillator hodoscope in combination with the front part of the EM calorimeter provides within a few nsec the first information on charged track hits with better than 5mm position accuracy and perhaps as low as 50 psec time accuracy. This could point to where in the drift chambers to start looking for tracks.

b) Next, the distant D.C.'s (4th station) have the lowest occupancy levels and tie nicely with the "charge" hodoscope information. Within 500 nsec one could identify space-time points with 2 nsec accuracy. Since the z-coordinate is not bent to first order, it would then be easy to start tracking by forming the 4th station track projections on 2 z-planes, the vertical (YZ) and horizontal (XZ) ones, which pass through the beams' nominal z-axis.

c) Subsequently, the formation of each of the XZ and YZ projections for say 30-40 tracks could proceed in parallel, starting from the outside ones and moving inwards onto the CCD's.

d) The CCD track projections are finally used to calculate the (x,y,z) coordinates of one or more vertices. Since the CCD's information consists of 3-dim space points, the 2 projections of each track are tied together, providing consistency and uniqueness of vertices.

The discussion above is only meant to suggest a direction to go:
Since the cleanest and fastest way to track seems to be with the outer part of the tracking system, one could "zoom in" from the outside onto the CCD's. Using outside tracking to aid the CCD's seems sensible. A detailed Monte Carlo study is needed to develop an optimal procedure and test the feasibility of this "zoom in" idea as a triggering method.

6. INVARIANT MASS TRIGGERS

Identifying a particle by measuring its mass through its decay into a dilepton or diphoton final state, like ψ ,Z $\rightarrow$ l+l-, would be possible with the EM calorimeter or the Muon system. We concentrate on the first here. 2nd Level invariant mass triggers seem to be an attractive possibility with our detector scheme for reasons specifically related to it:
a) The large distance (7m) of the EM calorimeter from the event vertex.
b) The superfast EM calorimetry with its excellent energy resolution and 3-dim segmentation could provide precise particle energies within 200 nsec.
c) The relatively small RMS error of 5(10) mm, which is possible for each electron (photon) using the "charge" hodoscope and/or the crude EM shower center estimate, also within 200 nsec.

The kinematics for such a trigger are favorable here. For example, for an e+e- decay the error for determining the mass, due to shower spacial resolution errors, has a broad maximum centered around the kinematic point where the 2 electron energies are equal, which is proportional to E/m: the higher the mass the better off we are, i.e. the higher the energy up to which we can obtain a certain mass resolution,

$$\frac{dm}{m}(D) = \frac{dD}{2*L} * \gamma = 5*10^{-4} * \gamma$$

where

dD = $\sqrt{2}$ * dx = 7 mm : the 2-shower transverse distance error
L = 7 m : the distance from the vertex
γ = E / m : energy to mass ratio of the resonance

In Table XI we note that for dm/m=.2 the energy range for Z$\longrightarrow$ e+e- is unlimited. But even for a π^0 it is up to 30 GeV, at which energy the 2 showers already merge considerably (distance =7cm) and a quick 2 separate shower identification may be already very difficult.

Thus, the problem reduces to that of a search for a pair of showers with the right mass (or distance). This trigger method looks quite promising and deserves further extensive study. The ψ- trigger would be rather difficult to implement, but if successful it should be extremely useful for several bottom and charm processes.

VII. L = 10**34/cm**2/sec POSSIBILITIES

The proposed detector could function near a luminosity of L=10**34 for several types of measurements:
1) Calorimetric missing Pt, jet measurements (Pt,m,E), crude multiplicities.
2) Muon Vector and E.
3) Isolated Electron Vector and E.
4) QGP crude dN/dy, E(EM-tot)/E(had-tot), dE/dy.
5) Low energy flavor identification with TOF+dE/dx (less than 5-10 GeV).
6) Drift Chamber Multiplicities.
7) Isolated Single Photon E and Vector.

The detector's central topology around y=0 is exactly matched with requirements for high L=10**34 : low-beta quads very close to interaction point (4-6 meters ?).

VIII. COSTS

Table XII gives crude estimates for all items summing up to about 680k readout channels and $108M cost. About 40% goes for BaF2 and scint.glass detectors. The Pb+gas calorimetry and muon-system follow with $18M and $10M.

Costs for most of the system seem to be quite stabilized and close to minimized. Only the fancy calorimetry material and the electronics for many channels are items that could experience significant cost reductions. For example replacement of BaF2 with scint.glass may result in close to $15M savings. Viewed in an orthogonal way, about $60M is for electronics, diodes and CCD's.

An absolute minimum of $70-80M for this kind of detector design and performance seems inescapable.

IX. CONCLUSIONS

1. MEASUREMENT CAPABILITIES

The scheme we advocate will have measurement capabilities, most of which a 4π device cannot match mostly due to scaling with distance from the beam, like particle identification, momentum resolution, TOF, occupancy/cell; or reduced backgrounds permiting the use of superior materials (BaF2), devices (CCD's, Diodes, RICH) and techniques (timing etc):

1) DP/P (electrons, photons) < 1.5% at all energies.
2) DP/P (hadrons, muons) = 2.5% * P (TeV).
3) Single photon vs. π^0 identification at least up to 1-2 TeV.
4) Electron identification in the middle of a high Pt jet core.
5) Hadron flavor identification with 0 <E(π)< 400GeV and 0 <E(K,p)< 650 GeV.
6) Jet flavor and its cascade identification up to E(jet) ~ 3-5 TeV.
7) At L= 10**34/cm**2/sec can do a small fraction of the physics possible below 10**33.
8) Good 2nd Level triggers for jets (E> 10GeV) and electrons (E> 1GeV).
9) 3rd Level triggers for $\psi \rightarrow l^+l^-$ (E> 10GeV) and $Z \rightarrow l^+l^-$ (E> 300GeV).
10) Some secondary vertex trigger capability at luminosities up to 10**32.

To implement this would require an effort not much smaller than that for a 4π detector, but would allow us to probe a considerable amount of important physics problems, which however are different and would be definitely inaccessible otherwise.

2. R & D NEEDED

We identify 4 R&D topics of critical importance for the realization of this detector scheme:

a) Develop a readout scheme for CCD's in a L=10**33 environment.

b) Readout efficiently the fast light component of BaF2 exclusively, using thin photodiodes.

c) Ongoing dense scint.glass development.

d) Testing a 6-7 L(al) long BaF2+Scint.Glass calorimeter prototype: measure its energy response to electrons and hadrons over a large dynamic energy range (100 MeV - 100 GeV) and with 10-100 nsec gates.

There are of course several R&D items discussed or simply identified in the past which would result in improvements of detector performance and physics capabilities, simplifications in detector design and operation and important cost savings, a typical example being a fast trigger processor for secondary vertices, in a 10**32 to 10**33 environment. We add 2 items of high importance, in our opinion:

a) A thin and very compact photomultiplier, with a few dynodes giving it gains of 100-1000, which could allow scint.glass to be used for the EM calorimeter as well, without the electronics noise dominating the energy resolution down to particle energies of 1 GeV.

b) Timing electronics with resolutions of a few picoseconds to take advantage of the fast light component of BaF2 for particle identification via the time of flight method.

3. OUTLOOK

We view our detector scheme here as a vehicle for a design philosophy study rather than as a specific and realistic detector design (it is probably too early for that), as we attempt to

a) define design criteria for best possible measurements attainable,

b) help identify critical R&D paths needed,

c) evaluate triggering capabilities and data acquisition and computing requirements,

d) study analytically, or with Monte Carlo simulations, signals for various processes using the design,

e) compare its performance to that of other specialized or general purpose 4π designs.

In this report we were able to address extensively (a) and (b) but made only a modest start on (c) and (d).

X. ACKNOWLEDGEMENTS

I would like to acknowledge important help from L.McLerran in understanding some physics concepts and valuable discussions with J.D.Bjorken and S.Majewski. I thank B.Cox and the other organizers of the Workshop for the challenging opportunity they gave us to try to come up with some new ideas in addressing outstanding problems.

XI. REFERENCES

1. G.J.VanDalen and J.Hauptman, "A Specialized High-Pt Spectrometer for the SSC" Proceedings of 1984 Summer Study on Design and Utilization of SSC, p.659.
2. V.Hagopian, "A Possible Specialized Detector Experiment for SSC", in the Summary Report of the PSSC Discussion Group Meetings (June, 1984).
3. F.Sciulli, "Report of the Specialized Detector Subgroup", in the Summary Report of the PSSC Discussion Group Meetings (June, 1984).
4. D.Loveless et al., "BOBO Oscillations at the SSC", Proceedings of the Chicago ANL Workshop on the $\bar{p}p$ Option on the SSC (Jan., 1984).
5. N.Giokaris and S.Majewski, "A 90° Spectrometer to Measure High-Pt Inclusive Charged Hadron Production and to Search for Parton Compositeness at SSC Energies", Proceedings of 1984 Summer Study on Design and Utilization of SSC, p.647.
6. J.W.Cronin et al., "Report of the Working Group on CP Violation and Rare Decays", Proceedings of 1984 Summer Study on Design and Utilization of SSC, p.161.
7. S.Errede, S.-H.Henry Tye et al., "Stable/Exotic Particle Production and Detection at the SSC", Proceedings of 1984 Summer Study on Design and Utilization of SSC, p.175.
8. M.S.Witherell et al., "Report of the Specialized Detector Group", Proceedings of 1984 Summer Study on Design and Utilization of SSC, p.643.
9. G.Arnison et al., "Charged Particle Multiplicity Distributions in Proton-Antiproton Collisions at 540 GeV Center of Mass Energy", Phys. Lett. 123B (1983) 108.
10. K.Alpgard et al (UA5 Collaboration), "Strange Particle Production at the CERN SPS Collider" Phys.Lett. 115B (1982) 65, and "Production of Photons and Search for Centauro Events at the SPS Collider" Phys.Lett. 115B (1982) 71.
11. G.Arnison et al., "Transverse Momentum Spectra for Charged Particles at the CERN Proton-Antiproton Collider", Phys. Lett. 118B (1982) 167.
12. G.J.Alner et al., "A New Empirical Regularity for Multiplicity Distributions in Place of KNO Scaling", CERN-EP/85-62.
13. F.E.Paige, "SSC Trigger Rate Estimates", see report in this Workshop.
14. W.Kononenko, G.E.Theodosiou et al., "Signal and Noise Measurements for Muons in Scintillating Glass with Vacuum Photodiode Readout", IEEE NS-31 (1984) 136.
15. I.I.Bigi, private communication.
16. H.E.Haber, "ζ's - A Probe of New W and Z Couplings", Proceedings of 1984 Summer Study on Design and Utilization of SSC, p.157.
17. H.E.Haber et al., "Signals of New W's and Z's", Proceedings of 1984 Summer Study on Design and Utilization of SSC, p.125.
18. C.Y.Chang and Z.M.Wang, "TOF for Heavy Stable Particle Identification", Proceedings of 1984 Summer Study on Design and Utilization of SSC, p.202.
19. L.D.McLerran and B.Svetitsky, Phys. Lett. 98B, 195 (1981); J.Kuti, J.Polonyi and K.Szlachnyi, Phys. Lett. 98B, 199 (1981).
20. J.Engels et al., Nucl. Phys. B205, 545 (1982) and L. Van Hove, Phys. Lett. 118B, 138 (1982).
21. T.H.Barnett et al., "Characteristics of JACEE Heavy Ion Events at Energies Above TeV/Nucleon"- Quark Matter '84 in Proceedings of the 4th International Conference on Ultra- Relativistic Nucleus- Nucleus Collisions, Helsinki, Finland, June 17-21, 1984, p.187.

22. E.V.Shuryak, Phys. Lett. 79B, 135 (1978).
23. M.A.Shifman et al.,Nucl. Phys. B147, 385 (1979).
24. J.Kogut et al., Phys. Rev. Lett. 48, 1140 (1982).
25. J.D.Bjorken, Fermilab Pub. 82/44-THY.
26. E.L.Feinberg, Nuovo Cimento 34A, 391 (1976).
27. E.V.Shuryak, "Non-Perturbative Phenomena in QCD Vacuum, and Quark-Gluon Plasma", CERN 83-01 (1 Feb. 1983).
28. L.J.Gutay et al., "Search for a Deconfined Quark Phase of Strongly Interacting Matter in $\bar{p}p$ Interactions at $\sqrt{s} \sim 2$ TeV", FNAL Collider Experiment No. E735 (April 11 1983).
29. B.Cox et al., "Uranium Liquid Argon Calorimetry: Preliminary Results from the DO Tests", Fermilab Conf. 86/14-E; presented at the DPF Meeting of the APS in Eugene, Oregon (August, 1985).
30. C.M.G.Lattes et al., "Hadronic Interactions of High Energy Cosmic-Rays Observed by Emulsion Chambers", Physics Reports 65 (1980) 151.
31. M.Althoff et al., "Determination of the Average Lifetime of Bottom Hadrons", Phys. Lett. 149B (1984) 524.
32. T.Ferbel and W.Molzon, Rev. Mod. Phys. 56, 181 (1984).
33. J.F.Owens et al., "High-Pt Photon Production and Compositeness at the SSC", Proceedings of 1984 Summer Study on Design and Utilization of SSC, p.218.
34. S.Matsuda and J.F.Owens, "Considerations for the Process pp→ W+photon+X at the SSC", Proceedings of 1984 Summer Study on Design and Utilization of SSC, p.216.
35. M.Laval et al., "BaF2: Inorganic Scintillator for Subnanosecond Timing", NIM 206 (1983) 169.
36. W.Kononenko et al., "Tests for a New Type of Calorimeter, the SPED", NIM 186 (1981) 585.
37. W.Selove and G.Theodosiou, "Scintillator Calorimetry With Vacuum Photodiode Readout", p.113; and "Calorimetry at L = 10**33", p.119, DPF Workshop on Collider Detectors: Present Capabilities and Future Possibilities, LBL (March, 1983).
38. V.Radeka, IEEE Transactions on Nuclear Science NS-24, 293 (1977).
39. B.Cox, "Possibilities for New Heavy Scintillation Glasses in Electromagnetic Hadron Calorimeters at the SSC", Proceedings of 1984 Summer Study on Design and Utilization of SSC, p.553.
40. G.E.Theodosiou et al., "Cherenkov and Scintillation Light Measurements with Scintillating Glass, SCG1C", IEEE NS-31 (1984) 57.
41. B.Pope et al., "Calorimetry: Working Group Summary Report", p.49, DPF Workshop on Collider Detectors: Present Capabilities and Future Possibilities, LBL (March, 1983).
42. W.W.M.Allison et al., "The Identification of Secondary Particles by Ionization Sampling (ISIS)", NIM 119 (1974) 499.
43. I.Lehraus et al., "Performance of a large scale multilayer ionization detector and its momentum use for measurements for the relativistic rise in the momentum range of 20-110 GeV/c", NIM 153 (1978) 347.
44. F.E.Paige and S.D.Protopopescu, "ISAJET: A Monte Carlo Event Generator for $\bar{p}p$ and pp Interactions", Version 5, BNL Report (June, 1985).
45. A.V.Kulikov et al., "Performance of the E715 Transition Radiation Detector", Proceedings of the DPF Santa Fe Meeting, Santa Fe (Nov., 1984).
46. B.Cox et al., "A Measurement of the Response of an SCG1-C Scintillation

Glass Shower Detector to 2-17.5 GeV Positrons" IEEE Trans. Nucl. Sci. NS-30, 127 (1983).
47. E.Eichten et al., "Supercollider Physics", Fermilab-Pub-84/17-T.
48. R.D.Field, "Jets and Event Topologies at the SSC", Proceedings of 1984 Summer Study on Design and Utilization of SSC, p.713.
49. T.Azemoon, "U-Gas Hadron Calorimeter for the L3 LEP Experiment", Gas Calorimetry Workshop at FNAL (Oct., 1985).
50. P.Constanta-Fanouraki et al., "A Microvertex Detector Proposal for the UA2 Experiment", Univ. of Pennsylvania Report UPR-134E (1984).
51. G.Theodosiou, "DO Microvertex Considerations..I", DO Note 140 (1984).
52. H.Satz, RHIC Workshop: Experiments for a Relativistic Heavy Ion Collider, BNL (March, 1985).
53. L.D.McLerran, private communication.
54. S.Aronson et al., "Design Report: The DO Experiment at the Fermilab $\bar{p}p$ Collider", FNAL (Nov., 1984).
55. G.Ciapetti et al. (UA1 Collaboration), "Average Pt Dependence on Event Charged Multiplicity in Min.Bias Events at S$\bar{p}p$S Collider", Proceedings of 5th Topical Workshop on $\bar{p}p$ Collider Physics", Saint-Vincent (Feb., 1985).
56. T.Ypsilantis, private communication and DELPHI Technical Proposal DELPHI 83-66/1, CERN/LEPC/83-3, LEPC/P2 (May 17, 1983).

XII. APPENDICES

1. MINIMUM BIAS AND LOW-PT JET EVENTS

A. Existing Data: Minimum bias data from UA1 and UA5 give

$$\sqrt{s} = 540 \text{ GeV}$$

$$\langle Nch \rangle = 29 \qquad \text{(Ref. 9)}$$

$$\langle Nn \rangle = 0.7 * \langle Nch \rangle \qquad \text{(Ref.10)}$$
$$\langle Nsn \rangle = \langle Nsch \rangle$$

$$dNch/dy = 3.5 \quad \text{in} \quad -2.5 < y < 2.5 \qquad \text{(Ref. 9)}$$

$$\langle Pt \rangle = 0.42 \text{ GeV/c} \qquad \text{(Ref.11)}$$

where
- Nn,Nch (Nsn,Nsch): No. of neutral and charged particles (strange particles)
- we count 1 neutral particle for every 2 photons.

Fig.1 shows DNch/Dy vs. $\sqrt{s}$ from Ref.9. Fig.2 shows how $\langle Pt \rangle$ increases both with $\sqrt{s}$ and with dN/dy (Ref.11). Furthermore cosmic shower data from E=10**12 to 10**15 eV (~SSC energy) show crude agreement with accelerator data on both $\langle N \rangle$ and $\langle Pt \rangle$ vs. $\sqrt{s}$ (Ref.30).

B. "Negative Binomial" Multiplicity Distribution: The UA5 1982 data, carefully analysed recently, are found to violate KNO scaling and obey a "negative binomial" distribution which has much larger fluctuations than KNO (Ref.12). This should not be so surprising since Feynman scaling, on which KNO is based, is violated. For $\langle N \rangle \gg k$, i.e. high energies, their distribution can be approximated by

$$\langle N \rangle * Pn = \frac{k^k}{\Gamma(k)} * z^{k-1} * e^{-k*z}$$

where $z = N / \langle N \rangle$
with moments: $C1 = 1$
$C2 = \langle N**2 \rangle / \langle N \rangle**2 \sim 1 + 1/k$

and with parametrizations

$$1/k = -.098(\pm.008) + .0282(\pm.0009) * \ln(s)$$

$$\langle N \rangle = 1.97(\pm 0.98) + 0.21(\pm 0.29) * \ln(s) + 0.148(\pm 0.022) * \ln^2(s)$$

Fig.3 shows C2-1 illustrating how "approximate" scaling, with moments independent of energy, was observed at lower energies.

C. Extrapolation to SSC Energies.

dNch/dy = 7.5 (UA1 data) + ("negative binomial") (Ref. 12)

$\langle Nn \rangle = 0.8 * \langle Nch \rangle$

$\langle Pt \rangle \; > 0.7$ GeV/c (CERN data vs $\sqrt{s}$ extrapolation) + (cosmics data)

σ(inel) = 100 mb --> 1 event / 10 nsec

Table I shows multiplicities, Pt and total Et= ΣPt produced in acceptances of Dϕ *Dy =1 and 3.2 str for 10, 100 and 1000 nsec gates along with their corresponding standard deviations calculated according to the negative binomial distribution. All we have done here is extrapolate Pt and Ntot from lower energy data, based on parametrizations of these data, exactly as we do with the inelastic cross section σ(inel).

These $\langle Pt \rangle$ estimates should be considered as lower limits
a) if cosmics data is right, indicating $\langle Pt \rangle > 0.7$ GeV/c at these energies,
b) if current trend of increasing $\langle Pt \rangle$ with dNch/dy continues and
c) if the strong relative increase of neutrals and strange production observed at 540 GeV continues.

D. Jet background extrapolations to SSC data.
Here the ISAJET Monte Carlo could be trusteed, as based on perturbative QCD calculations, which are rather well understood theoretically and whose predictions were in striking agreement with the CERN data at $\sqrt{s}$= 540GeV.

Fig.4, taken from F.Paige's contribution to this Workshop (Ref.13), gives the total cross section (mb) for 1,2,..,6 jet events vs minimum Pt/jet, using a "DR=1" trigger acceptance, which is about the same with our Dϕ *Dy=1. For Et(jet)> 10 GeV we estimate aσ = 5mb. If we fold in our detector acceptance and estimate the rate for detecting a jet with Pt> 10GeV coming from any jet-event (1,..,6 jets), we find that on the average we must see 2 jets, each with $\langle Pt \rangle$= 15 GeV/c within 3 strs per 1 μsec. So we must add a Pt= 30 GeV/c to the 480 GeV/c from min.bias interactions.

2. QUARK GLUON PLASMA

Here, we use the concepts of the QCD vacuum with its energy density fluctuations, illustrated for a proton in Fig.9 (Ref.27), of a phase transition to a plasma of current quarks and gluons the "elementary constituents" shown in Fig.10 (Ref.20) & 11 (Ref.21), and the thermodynamic evolution of such a plasma, heating with compression and cooling with expansion. From the uncertainty principle, we can determine both
a) the spacial extent of a fluctuation or the size of the corresponding particle from the intrinsic "Fermi" momentum of its constituents, hadronizing into jets, or from the mass of constituent pairs annihilating into dileptons,
b) the strength of these fluctuations or energy density of matter from the Pt-spectrum of the corresponding constituents' hard scattering at very short distances.
For example, appearence of jet intrinsic $\langle Qt \rangle \sim$ 10-100 GeV/c or high rates of direct photons with Pt> 2 TeV, as shown in Fig.5b, could signal current quark compositeness.

If enough energy is supplied locally (high energy density, ε) and fast, so that temperature (T) doesn't have time to rise considerably, then the entropy density (S), which is proportional to the multiplicity density dN/dy, might undergo a finite jump, i.e. a 1st order phase transition, and become high enough to initiate a plasma (Ref.28),

$$\varepsilon = E/V \quad (GeV/fm^{**}3) \; ; \qquad T \sim Pt$$

$$S = \varepsilon/T \sim dn/dy$$

The temperature of an ensemble of constituents is related to their "Fermi" momentum <Qt> and hence the size of the boundaries in which they exist. It may make sense then to assume that a phase transition to a plasma of current quarks and gluons, in the picture of Fig.9, could occur near a temperature corresponding to the "constituent quark" size:
The nucleon is known experimentally to have a radius of about 1 fm. Assuming its volume is totally occupied by 3 "constituent quarks" (Fig.9), the position uncertainty of elementary constituents (current quarks and gluons) inside each "constituent quark" would be about 1.1 fm. Using the uncertainty principle we obtain an intrinsic "Fermi" momentum or a temperature ~180 MeV.

Theoretical lattice gauge calculations of QCD predict a phase transition from hadrons to a quark-gluon plasma at sufficiently high temperatures and/or quark densities (Ref.19). Fig.10 shows such a result (Ref.20): a transition around T ~ 215 MeV.

The higher the temperature of the phase transition, the higher the required energy density to be supplied for producing an adequate increase in entropy density. For example, QCD-vacuum phenomenological calculations (Ref.22 & 23) estimate the strengths of energy density fluctuations for the vacuum's "constituent quarks" and for hadron bags of Fig.9 and find them to be about an order of magnitude apart:

$$\varepsilon(vac) = -500 \; MeV/fm^{**}3 \sim (10 \text{ to } 20) * \varepsilon(bag)$$

In fact another lattice gauge calculation, using SU3 color fields, produces two phase transitions with typical energy densities an order of magnitude apart (Ref.24).

We can estimate crudely the energy density at $\sqrt{s}$= 40 TeV, using J.D.Bjorken's (Ref.25) 1-dim model and our SSC extrapolations above,

$$\varepsilon = 0.32 * dNch/dy \quad [GeV/fm^{**}3]$$

If the "negative binomial" multiplicity distribution were to hold up to 40 TeV, we can calculate a cross section vs. a lower limit of ε, shown in Fig.12. For example the cross section for events with ε > 7.5 GeV/fm**3 would be close to 2mb. This is about 2.5-3.0 times the estimated density for the supposed plasma ignition to commence in the JACEE data (Fig.11) and in theoretical calculations (Ref.52). With such high energy densities and rates centrally produced, decisive tests of QGP ideas may become possible.

TABLE I. MINIMUM BIAS BACKGROUND ESTIMATES

GATE (nsec)	ACCEPTANCE (str)	N events	Nn neutral	Nch charged	Nt total	C2*Nt/ N (2nd mom)	Pt (GeV/c)
10	3.2	1	3.0	3.7	6.7	+ 20	4.8 + 14
100	"	10	30	37	67	+ 63	48 + 45
1000	"	100	296	370	666	+200	480 +145
10	1.0	1	0.9	1.2	2.1	+6.3	1.5 +4.5
100	"	10	9.3	12	21	+ 20	15 + 14
1000	"	100	93	116	209	+ 62	150 + 45

TABLE II. CALORIMETER ENERGY RESOLUTION CHARACTERISTICS

Calorimeter Section	Material + Readout	Preamplifier t(r) (nsec)	Preamplifier Noise (electrons)	Noise / Signal 1 GeV e	1 GeV h	10 GeV e	10 GeV h
E-M	BaF2 + Diodes	5	5000	~ 2%	7%	.3%	.7%
HADRON	S.Glass + "	20	2500	-	110%	-	11%
LEAKAGE	Pb + gass	100	1160	-	-	-	-
Total				2%	60%	.3%	6%
Intrinsic Photostatistics Resolution				1.5%	55%	1%	16%

TABLE III. CALORIMETRIC TRIGGERS AND MIN. BIAS BACKGROUNDS

PARAMETER	TOTAL	E.M.	HADRON	LEAKAGE
Length (L(al))	13	1.5	5.5	6.0
Gate (nsec)		10	50	200
Noise = Minimum Bias Background ($D\phi$ = Dy = 1) (*)				
Energy fraction	1.0	.74	.26	.002
Energy (GeV)	3.1	1.1	1.95	.05
Jet Triggers ($D\phi$ = Dy = 1)				
Energy (GeV)	10 GeV	6.5	3.5	.03
<Noise>/Signal	.23	.17	.56	.60
40% / $\sqrt{E}$	.13			
Energy (GeV)	100 GeV	63	35	2
<Noise>/Signal	.02	.018	.056	.025
40% / $\sqrt{E}$	.04			
Electron Triggers ($D\phi$ *Dy = 4x10**-4 : 16 blocks of 3cmx3cm)				
Energy (GeV)	1 GeV	.99	.01	0
<Noise>/Signal	1.4x10**-3	6x10**-4	1.3x10**-1	0
1% / $\sqrt{E}$	1x10**-2			
Energy (GeV)	10 GeV	9	1	0
<Noise>/Signal	1.4x10**-4	6.5x10**-5	1.3x10**-3	0
1% / $\sqrt{E}$	3x10**-3			
Hadron Triggers ($D\phi$ *Dy = 3.6*10**-3 : 16 blocks of 9cmx9cm)				
Energy (GeV)	10 GeV	3.0	6.5	.5
<Noise>/Signal	~ 10**-3	1.4x10**-3	1.1x10**-3	3.6x10**-4
40% / $\sqrt{E}$	0.13			

(*) At L = 10**33/cm**2/sec

TABLE IV. CCD VERTEX DETECTOR

Station #	1	2	3	
Distance from IR (cm)	1	10	15	
Planes/Station	2	2	2	
Area/plane (cm**2)	2x10	15x25	22x37	
Site size (μm**2)	20x20	20x20	40x40	
#Sites/plane (10**6)	5	~ 90	~ 200	
Singles Rate (Hz/site)	~ 500	5	2	(*)

(*) For minimum bias events at L=10**33/cm**2/sec

TABLE V. DRIFT CHAMBER PARAMETERS

Station #	1	2	3	4	
Distance from IR (m)	0.4	0.8	1.4	6.7	
# of Modules	1	1	1	4	8
# Planes/Module	15X	15X	15X	15X	15X
(10wires+5strips)	15Y	15Y	15Y	15Y	15Y
Area (m**2)	.6x.6	2x2	4x4	4x4	1.5x4
Singles Rates(*) (kHz/wire)	~ 1200	~ 720	~ 360	~ 80	80
Sense-Cathode Distance (mm)	1	2	2	5	
Resolution (μm)	100	100	150	150	
# of Wires	9000	15000	12000	48000	36000

(*) For minimum bias events at L=10**33/cm**2/sec and magnet off

TABLE VI. RING IMAGING CHERENKOV COUNTER

A). RADIATOR		
Length (m)	4	
Solid Angle	Dy = Dϕ = +-0.5	
Gas and Pressure	95% He + 5% CF4 @ 1Atm	
Spherical Mirror Size (m**2) (2 pieces)	2 of 6x3 (ZxY)	
Spherical Mirror Radius (m)	8	
Threshold for π's (GeV)	15	
Angular Resolution (mrad)	0.3	
NO (Figure of Merit)	150	(1)
Charged Particle Rate (Hz) (inside the radiator)	10**8	(2)
B). PHOTON DETECTOR		
# of Modules	2	
Optical Window	CaF2	
Photoagent Gas (at 1 Atm)	(He + 20%CH4 + 1%H2) + 0.3Torr TMAE	
Gain (e/photon)	3x10**5	
Readout	Cathode wedge and strip pads with FADC's	
Active Surface(m**2) (each module)	0.6 x 1.0	
Spatial Resolution-RMS (mm)	0.8	
# photoelectrons (asymptotic)	7	
Separation Range (GeV) (3)	π/K : 15 -> 390 K/p : 50 -> 650	
Active Gas Layer Thickness (cm)	2.5	
# of Wedge & Strip Pads (each module)	500	
# of FADC's (each module)	1500	
Rate Limit (MHz)	1	

(1) Number of detected photons: $N = NO*L*(\sin(\theta))^{**2}$
where L = Length of Radiator
θ = Cherenkov Light Angle

(2) Assume : Luminosity = 10**33/cm**2/sec
Inelastic Cross-Section @ 40TeV = 100 mb
Charged Particle Multiplicity, dNch/dy = 7.5 (magnet off)

(3) Assumes that momentum has been measured with an accuracy of 10% or better and a minimum number of 3 photoelectrons has been detected (lower limit) and the mean Cherenkov light rings' radii for the two hypotheses differ by more than 3rms of the spatial resolution. Also we have assumed that there are less than 5 photoelectrons per event per pad.

TABLE VII. TRANSITION RADIATION DETECTOR

Distance from IR (m)	6.2
# of Modules/station	8
Radiator	
-material	Polypropylene
-area (m**2)	6x6
-# of layers/module	200
-foil thickness (μm)	17
-foil separation (mm)	0.5
PWC	
-gas mixture	70%Xe + 30%CH4
-cathode-anode distance (mm)	5
-drift time (nsec)	220
-threshold (keV)	6.5
-# of sense wires/PWC	3,000
-singles rates (Hz/wire)	1.9x10**4 (*)
Total Length	
(m)	0.9
(L(rl))	0.06

(*) For minimum bias events at L=10**33/cm**2/sec

TABLE VIII. CALORIMETER PARAMETERS -- CENTRAL REGION

PARAMETER	E-M	HADRON	LEAKAGE
Acceptance:	($D\phi$ = 1) x (Dy = 1)		
Absorber	BaF2	Scint. Glass	Pb
Active Converter	BaF2	Scint. Glass	Gas
Depth (L(rl))	20		
(L(al))	1.5	5.5	6.0
Longitudinal Segmentation:			
Sampling (L(rl))	"continuous"	"continuous"	4 & 8
No. of Readouts	5	4	3
Transverse:			
Tower Area			
(cmxcm)	3 x 3	9 x 9	10 x 10
($D\phi$ xDy)	4.3mr x .004	13mr x .013	13mr x .013
No. of Towers	40k	4.4k	4.4k
Readout:			
Technique	Photoelectron Conversion	Photoelectron Conversion	Prop. Charge Multiplication
Device	Diodes	Diodes	Gas Tubes
Gate (nsec)	5-10	50-70	200
No. of Channels	200k	18k	13k

TABLE IX. CALORIMETER PARAMETERS -- OUTER REGION

PARAMETER	E-M	HADRON	LEAKAGE
Ring Acceptance:	($D\phi$ = 0.4) x (Dy = 0.4)		
Absorber	Pb	Pb	Pb
Active Converter	Gas	Gas	Gas
Depth:			
(Lr.l.)	20		
(La.l.)	0.7	6.3	5.0
Longitudinal Segmentation:			
Sampling (Lr.l.)	1/4	1.5	4 & 8
No. of Readouts	4	4	2
Transverse Segmentation:			
Tower Size			
(cmxcm)	4 x 4	12 x 12	13 x 13
($D\phi$ xDy)	5.7mr x .006	17mr x .017	17mr x .017
No. of Towers	36k	4k	4k
Readout Technique	Photoelectron Conversion	Photoelectron Conversion	Prop.Charge Multiplication
Device	Diodes	Diodes	Gas Tubes
Gate (nsec)	50	100	200
No. of Channels	144k	16k	8k

TABLE X. 1-JET EVENT RATES

Pt Threshold (GeV/c)	Rate(*) (Hz)	Integrated Luminosity (crossings/cm**2)	Total No of Jets
100	16*10**1	10**40	158x10**7
250	8*10**0	"	8x10**7
500	6*10**-1	"	6x10**6
1,000	5*10**-2	"	5x10**5
1,500	5*10**-3	"	5x10**4
2,000	7*10**-4	"	7x10**3
4,000		10**41	2x10**2
10,000		"	< 1x10**0

(*) At L= 10**33/cm**2/sec and Acceptance(jet axis)= 0.36str

TABLE XI. INVARIANT MASS RESOLUTION AND DECAY KINEMATICS

Particle	Mass (GeV)	Dm/m	Separation (cm)	Energy (GeV)
Z	92.9	.05	14	9290
Y(1S)	9.5	.1	7	1890
J/ψ	3.1	.1	7	620
ϕ	1.0	.1	7	200
π	0.14	.2	7	30

TABLE XII. JET SPECTROMETER READOUT COUNT AND COSTS

ITEM	READOUT CHANNELS (k)		COSTS ($M)
TRACKING:			
CCD's	3	(processors)	4.5
Drift Chambers	120		11.0
SOLENOIDS			3.0
TRD	32		4.0
RICH:			
Gas Detector	4		1.0
SCINT.HODOSCOPES:			
dE/dx + TOF	100		7.0
CALORIMETRY:			
BaF2	200		35.0
Scint. Glass	20		9.0
Pb + Gas	170		18.0
MUONS:			
Toroids			8.0
PWC's	30		2.0
TRIGGERING:			
Processors			5.0
TOTALS	~ 680k Channels		~ $ 108 M

Reference 9

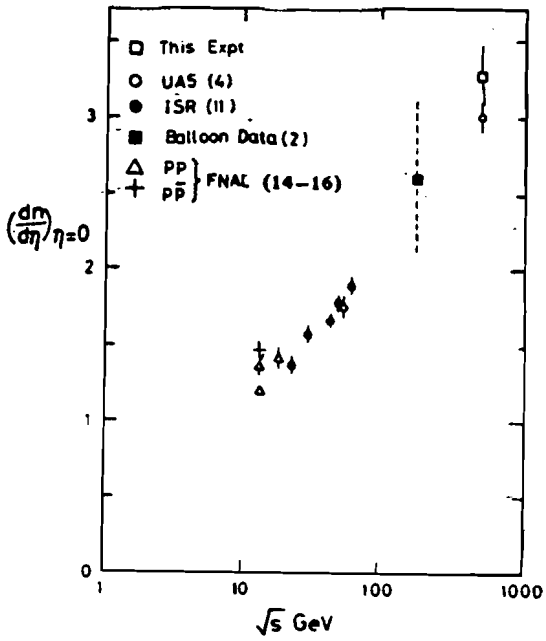

The central pseudo-rapidity density for this and other experiments as a function of centre of mass energy $s^{1/2}$.

Figure 1

Reference 11

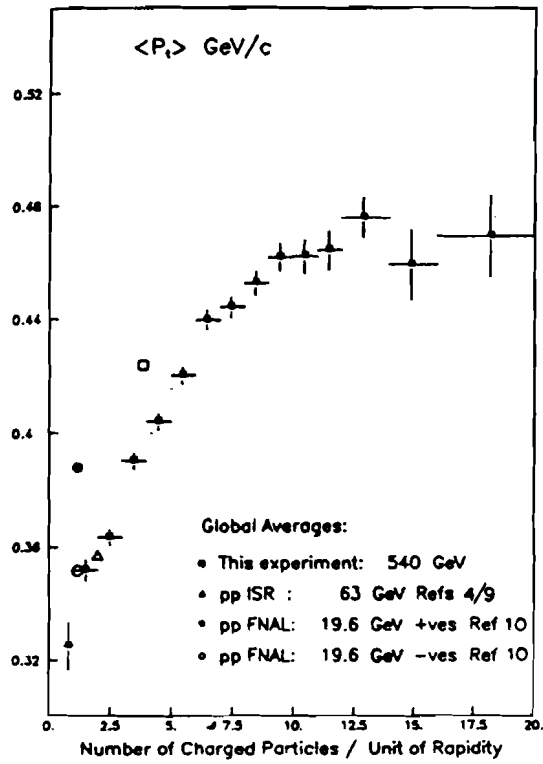

The mean transverse momentum of charged hadrons ($\sqrt{s}$ = 540 GeV) as a function of charged track multiplicity in the rapidity interval $|y| < 2.5$ (Error bars are purely statistical. Systematic effects from acceptance and fitting procedures could alter the $\langle p_t \rangle$ scale by up to 10 MeV/c. Points without error bars give the global average of p_t as a function of the *mean* number of charged particles per unit of rapidity at FNAL ISR and collider energies).

Figure 2

Reference 12

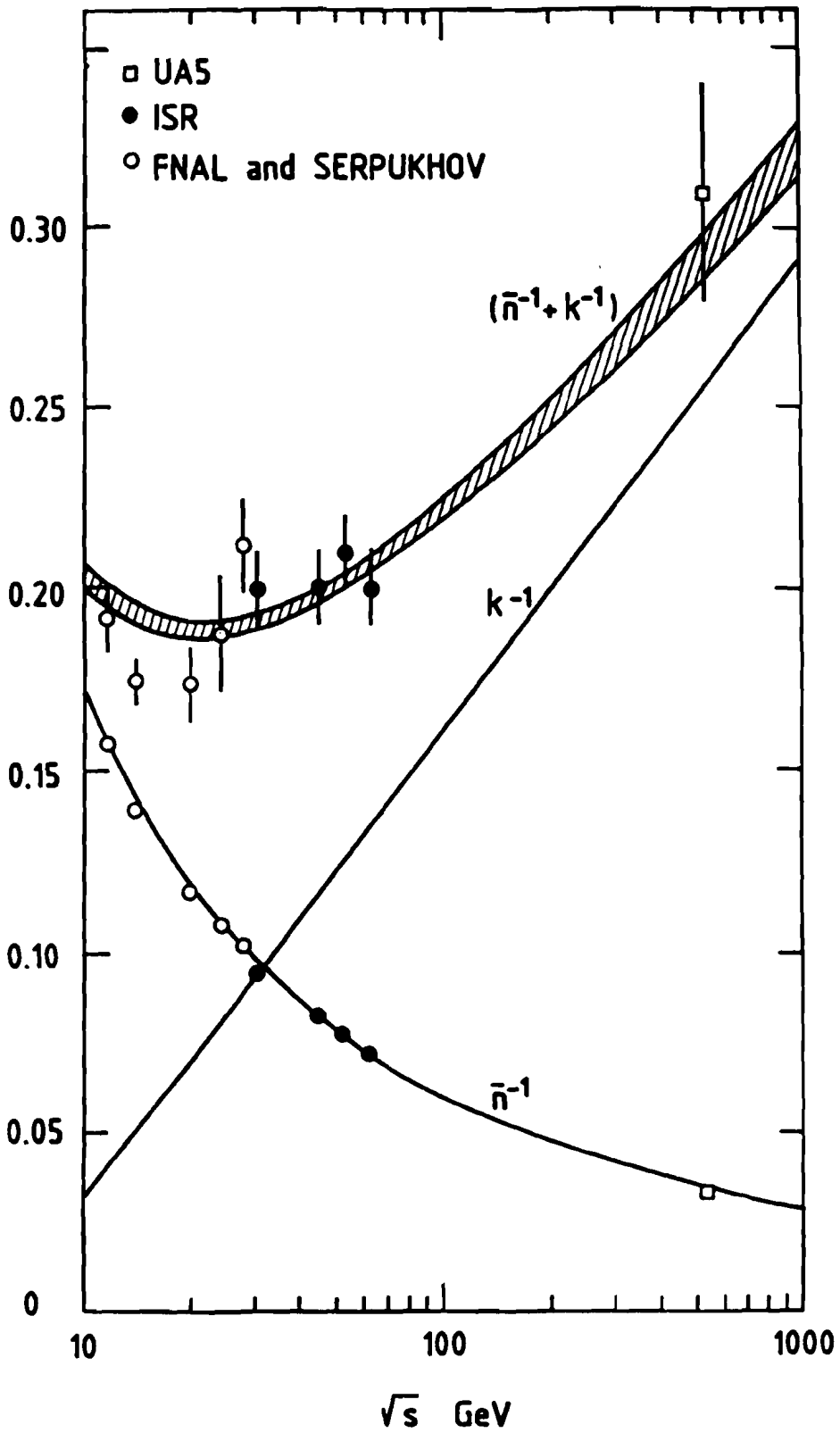

Figure 3

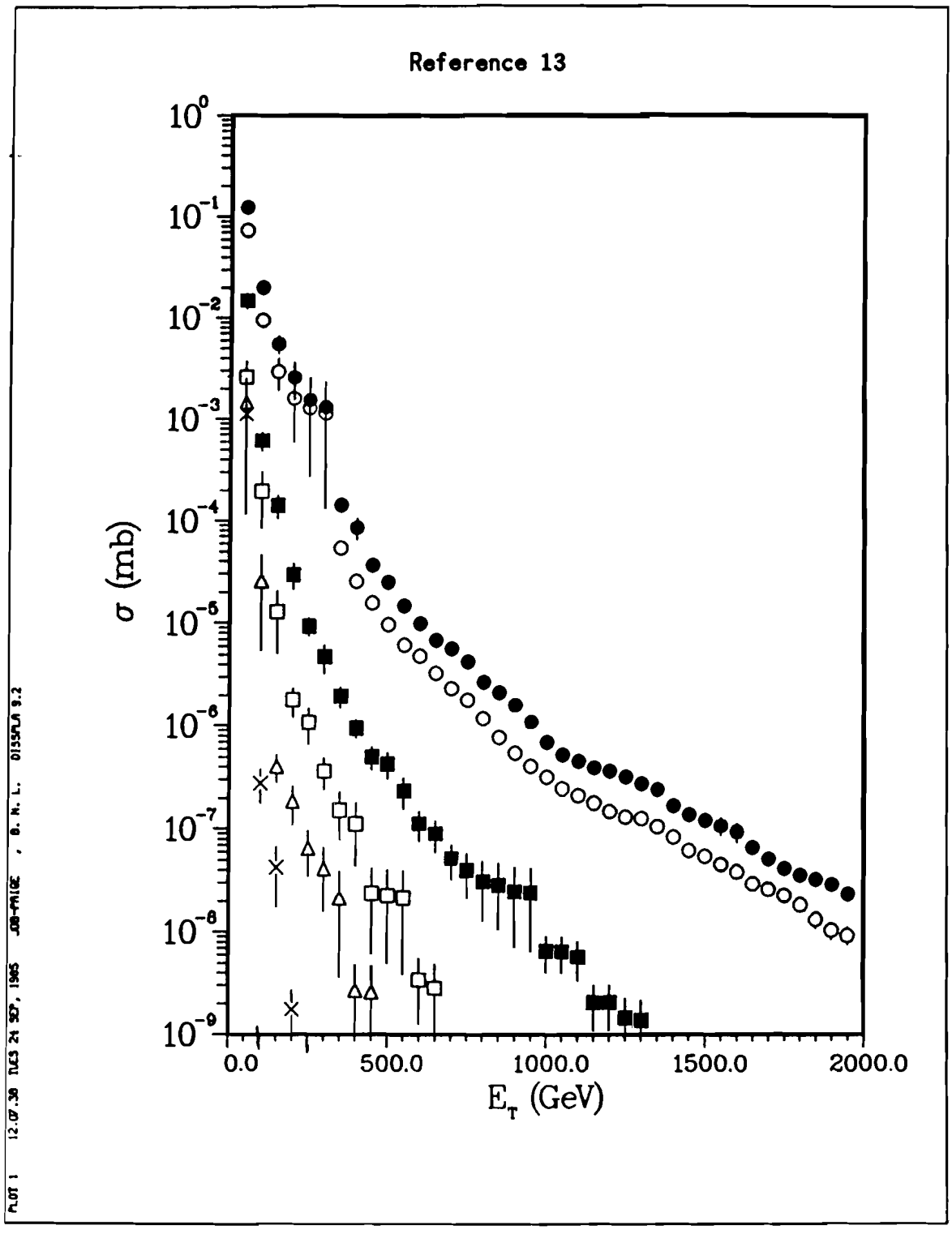

Cross sections for 1, 2, 3, 4, 5, and 6 jets vs. the minimum E_T of a jet, using $\Delta R = 1.0$ for the clustering.

Figure 4

Reference 33

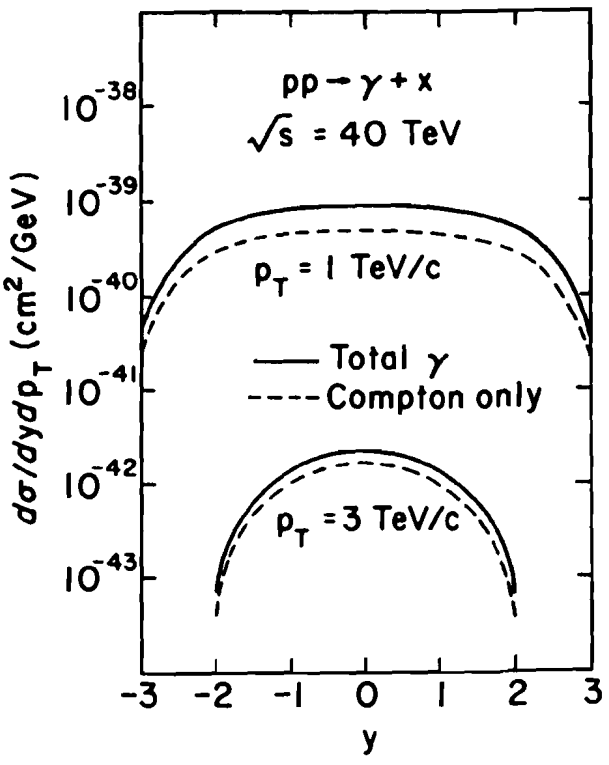

Predictions for $d\sigma/dydp_T$ for Υ production at p_T = 1 TeV/c and 3 TeV/c.

Figure 5a

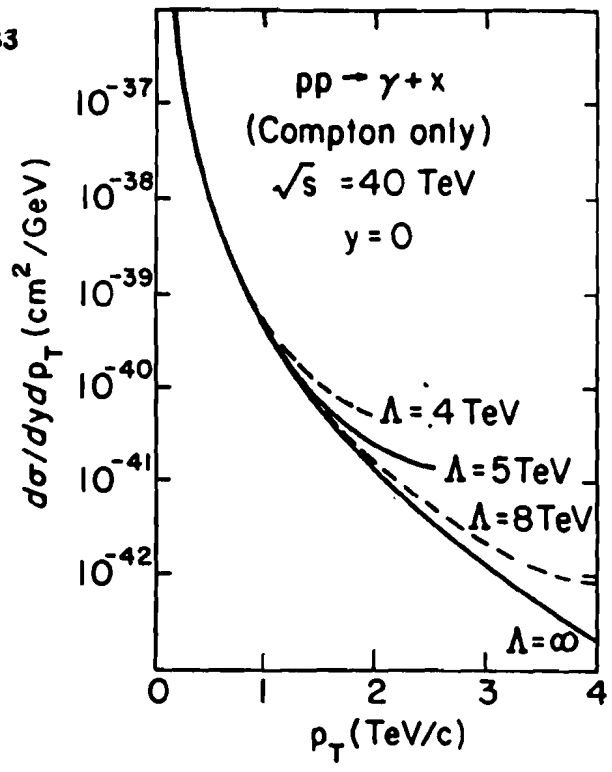

Predictions for $d\sigma/dydp_T$ based on the Compton process, modified to include effects of compositeness. Results are shown for $\Lambda = \infty$, 8, 5 and 4 TeV.

Figure 5b

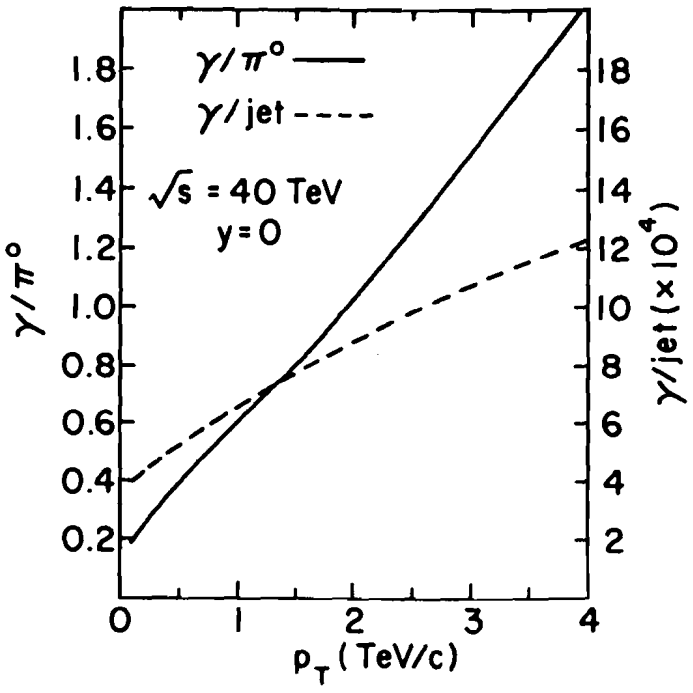

Predictions for the Υ/jet and Υ/π^0 ratios

Figure 5c

Reference 34

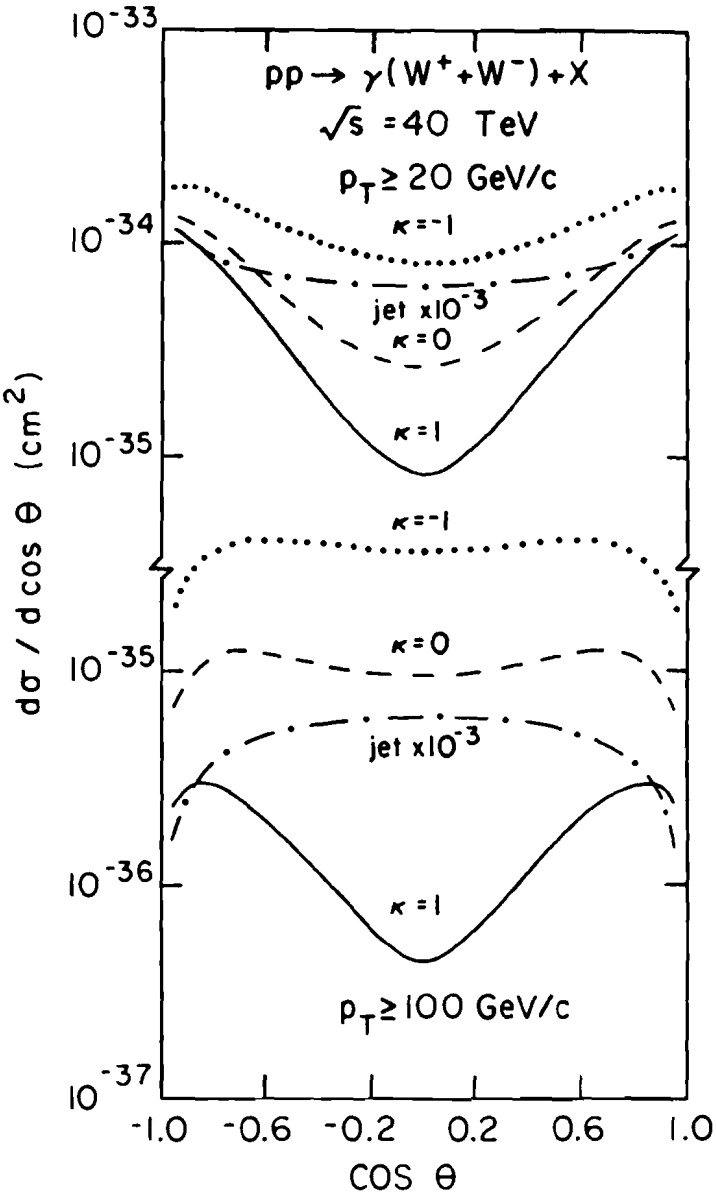

Predictions for the angular distribution of the W boson in the Wγ rest frame for κ=-1,0, and 1. The contributions expected from the background subprocesses are shown by dash-dotted lines after being reduced by a factor of 1000.

Figure 6

Reference 16

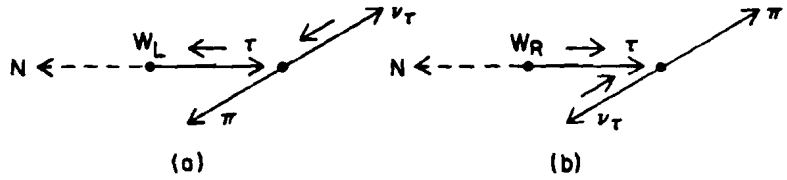

Schematic view of the sequential decay $W_{L,R} \to \tau N$, $\tau \to \pi\nu_\tau$. The arrows above the τ and ν_τ denote helicity. The ν_τ is always left-handed; the τ helicity depends on the nature of the W as shown. Angular momentum conservation demands that the configurations shown above are the ones favored.

Figure 7a

Reference 17

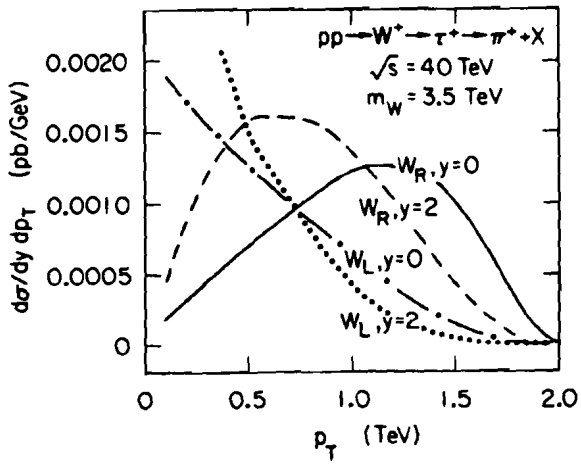

Single π^+ p_T-spectra at $\sqrt{s} = 40$ TeV from the sequential decay $W^+ \to \tau^+ \to \pi^+$.

Figure 7b

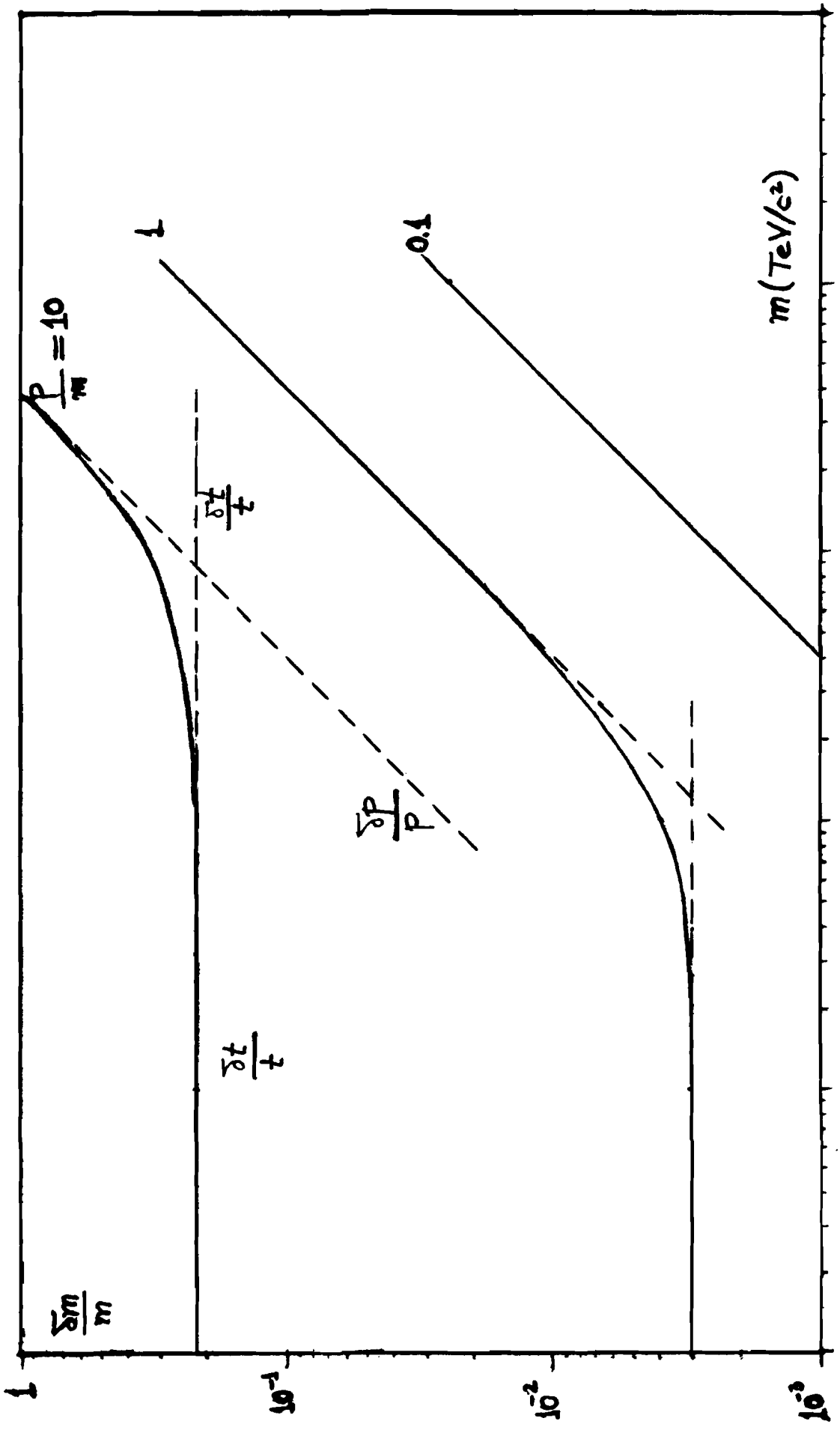
$\frac{\Sigma m}{m}$
1
10^{-1}
10^{-2}
10^{-3}
$\frac{p}{m}=10$
1
0.1
$\frac{\sigma_p}{p}$
$\frac{\sigma_p}{p}$
$\frac{\delta p}{p}$
m(TeV/c²)
10.0
1.0
0.1
0.01

Figure 8

Reference 27

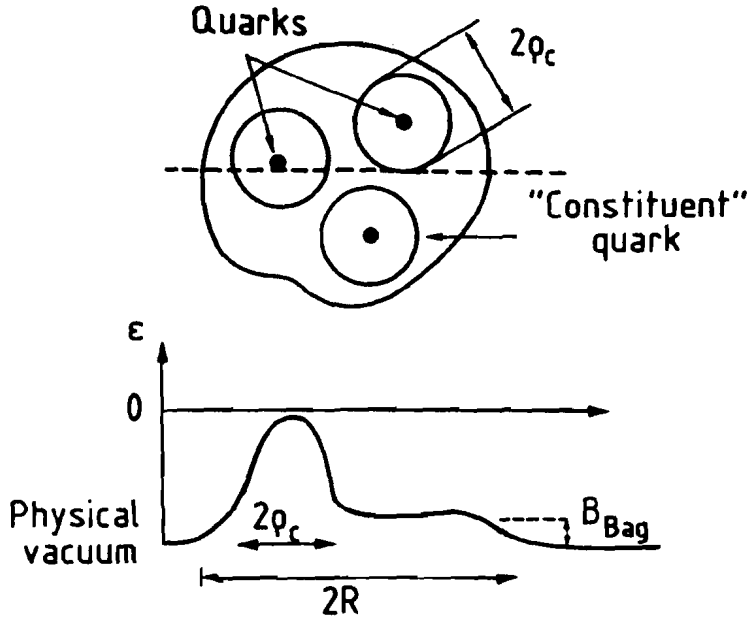

Schematic picture of the energy density distribution in the proton according to the "two-component model" along the diameter shown by the dashed curve in the upper part of the figure.

Figure 9

Reference 20

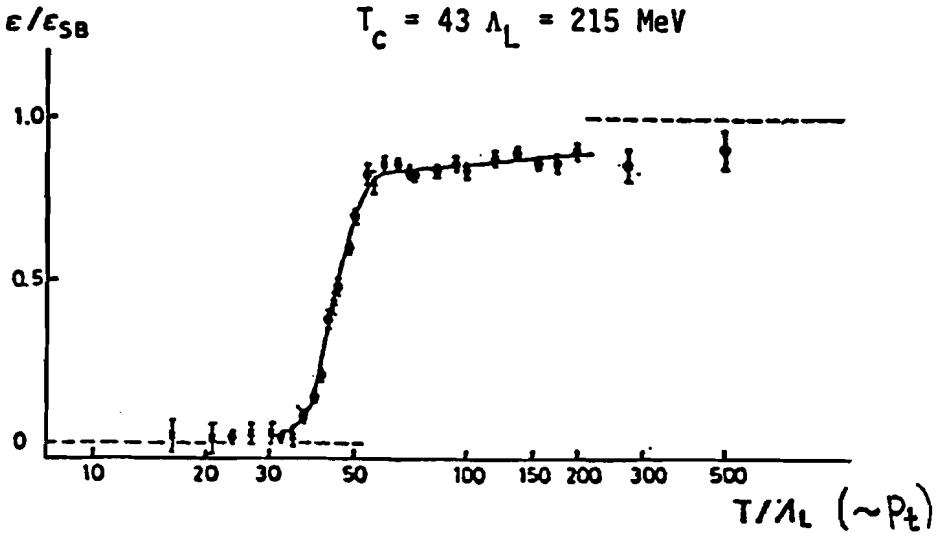

Figure 10

Reference 21

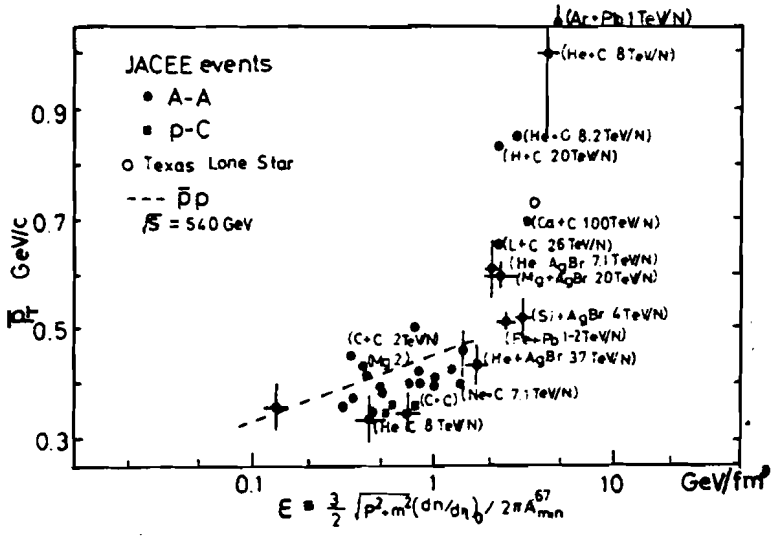

Figure 11

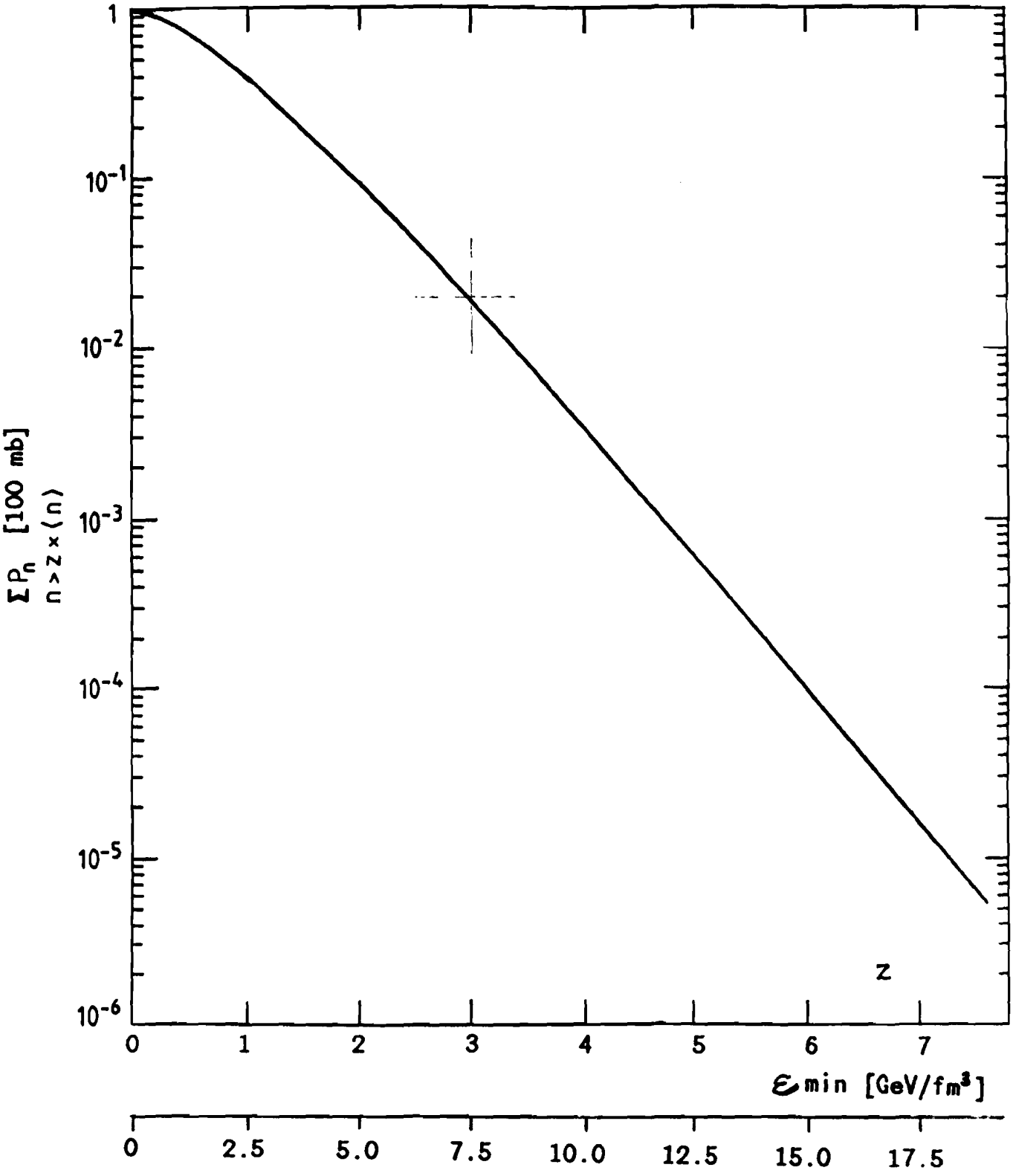
1
10^{-1}
10^{-2}
10^{-3}
10^{-4}
10^{-5}
10^{-6}
ΣP_n [100 mb]
$n > z \times \langle n \rangle$
z
0
1
2
3
4
5
6
7
ε min [GeV/fm^3]
0
2.5
5.0
7.5
10.0
12.5
15.0
17.5

Figure 12

Reference 35

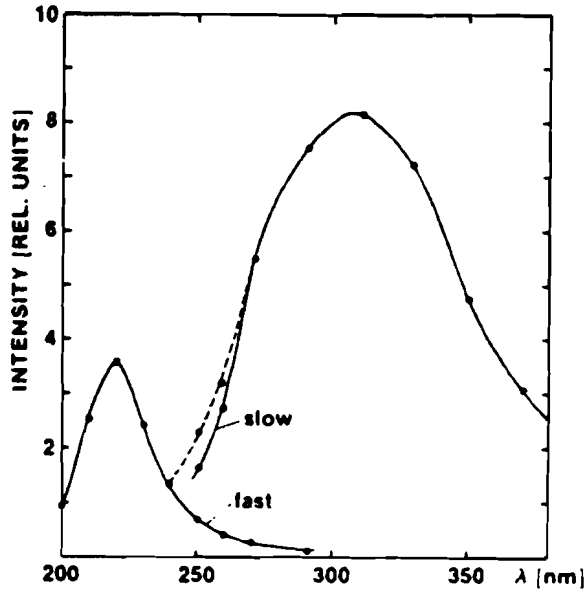

Time-resolved emission spectrum of the BaF_2 crystal. The relative intensity of the fast and slow components were normalised based on an analysis of the light pulse shape, see text for details. The spectrum is corrected for the efficiency of the grating in the monochromator and for the quantum efficiency of the XP 2020 Q photomultiplier.

Figure 13

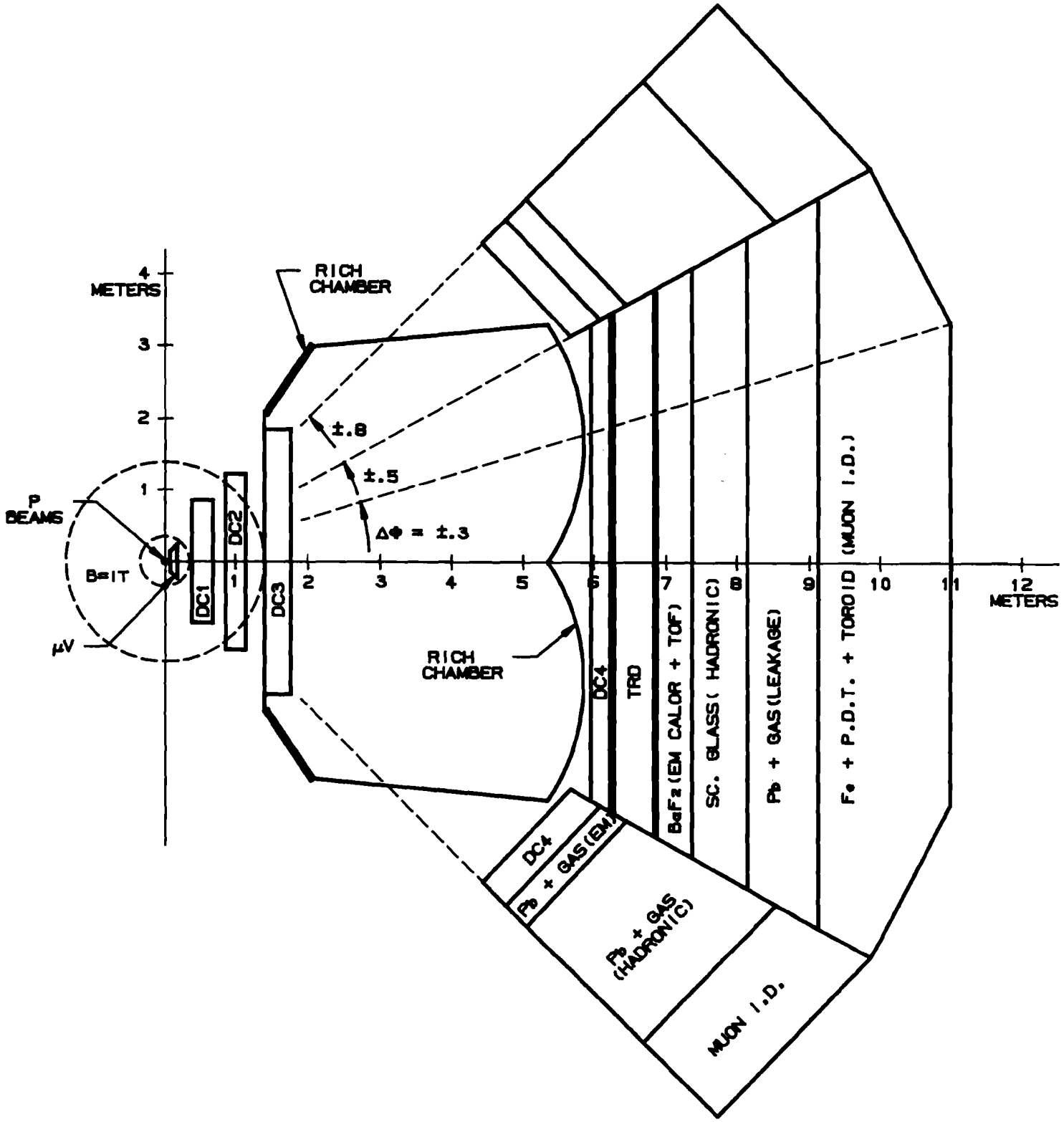
4
METERS
3
2
1
RICH
CHAMBER
±.8
±.5
Δφ = ±.3
P
BEAMS
B=IT
μV
DC1
DC2
DC3
1
2
3
4
5
6
7
8
9
10
11
12
METERS
RICH
CHAMBER
DC4
TRD
BaF2 (EM CALOR + TOF)
SC. GLASS (HADRONIC)
Pb + GAS (LEAKAGE)
Fe + P.D.T. + TOROID (MUON I.D.)
DC4
Pb + GAS (EM)
Pb + GAS
(HADRONIC)
MUON I.D.

Figure 14

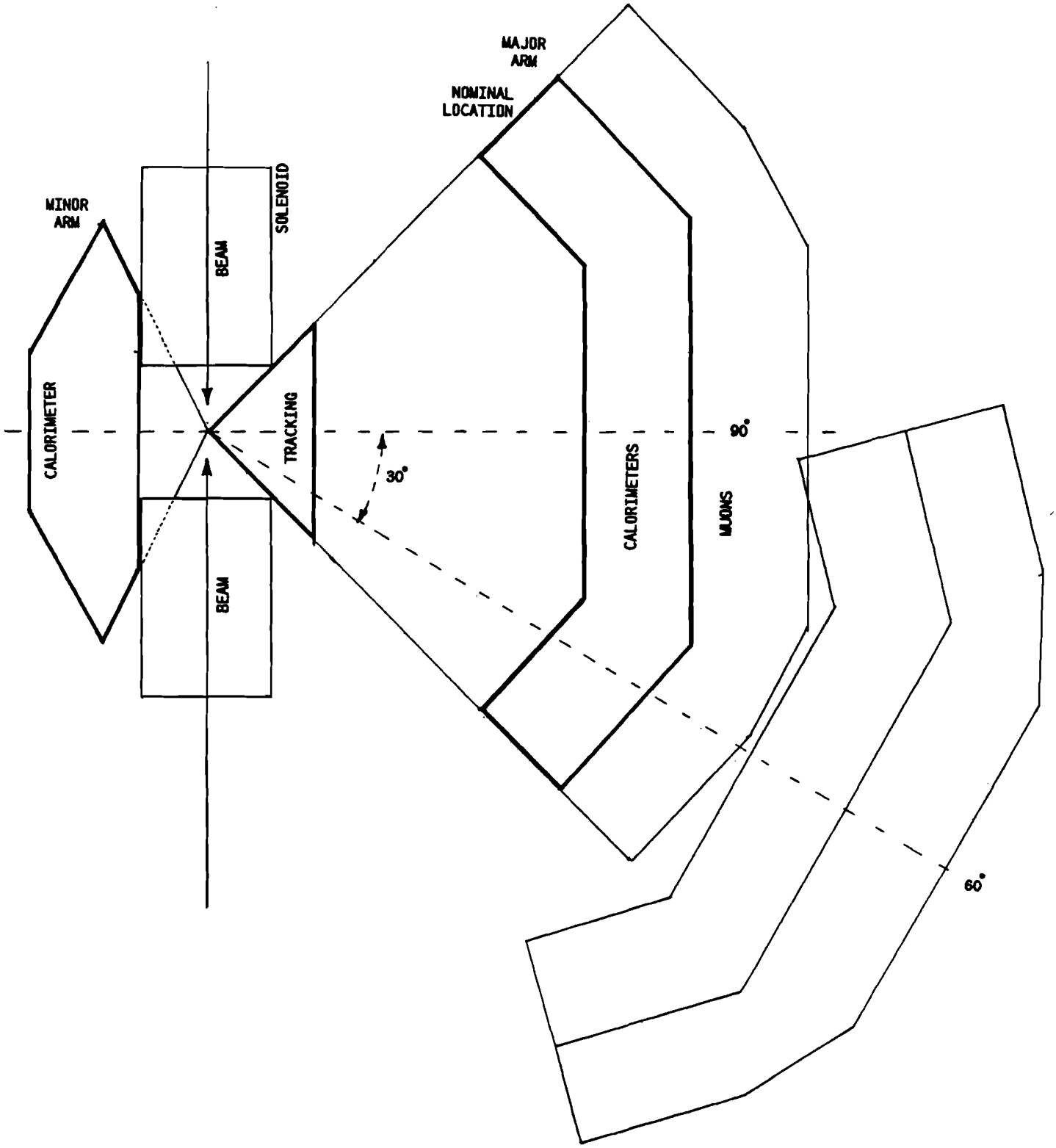

SPECTROMETER BEAM-PLANE VIEW :

Rapidity coverage at nominal location (symm. axis θ θ= 90° and calorimeter distance = 7 meters) and at another one, rotated by 30 and moved to a longer distance from the interaction region by 4.7 meters.

Figure 15

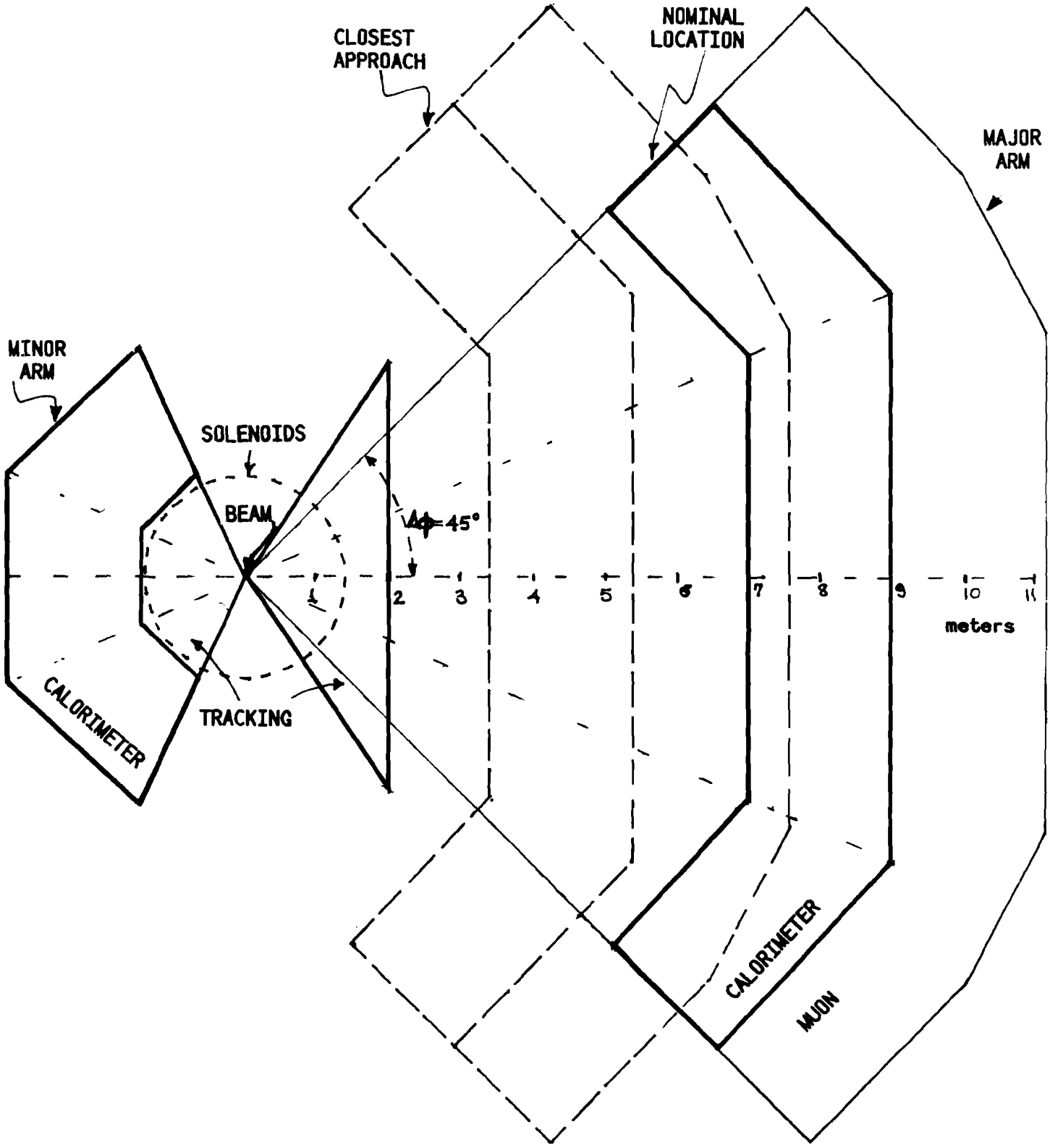

SPECTROMETER TRANSVERSE PROFILE :

Azimuthal Coverage at the nominal location (symm. axis @ $\theta = 90^\circ$ and calorimeter distance = 7 meters) and "zoomed in" with the calorimeter starting at half the nominal distance.

Figure 16

Reference 42

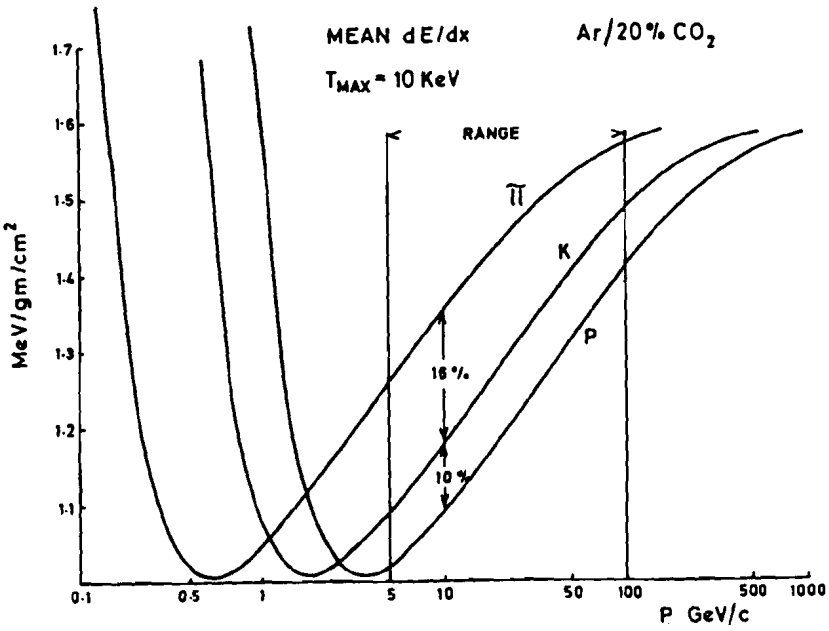

The ionisation loss in argon + 20% CO_2 at atmospheric pressure for π, K and p based on the formula of Sternheimer and Peierls

Figure 17

Reference 45

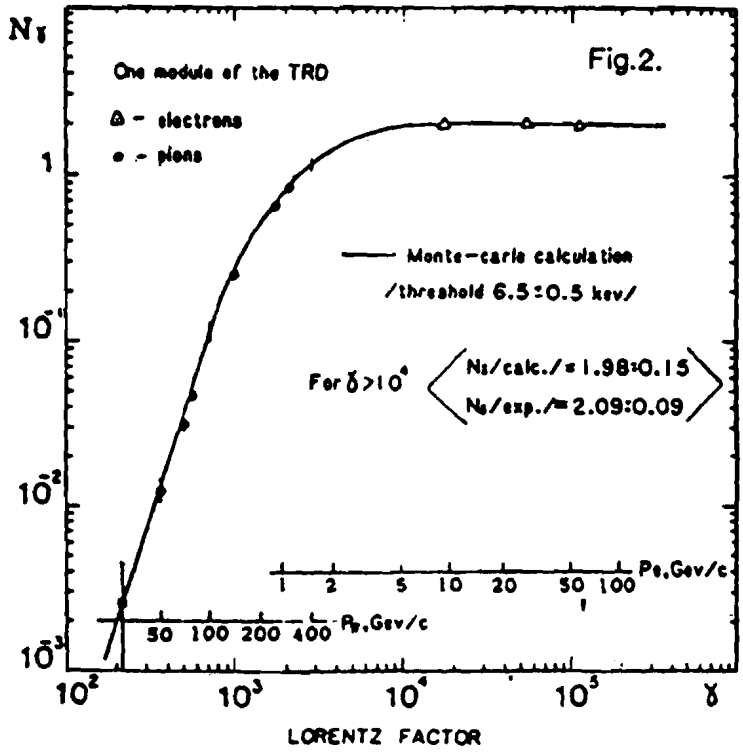

Figure 18